Chapter II: Ligand-capped heterogeneous catalysts from groups 8-10

María Dolores Fernández-Martínez, Cyril Godard
e-mail: cyril.godard@urv.cat
Departament de Química Física i Inorgánica, Universitat Rovira i Virgili, C/ Marcel·lí Domingo 1, Campus Sescelades, Tarragona 43007, Spain

Graphical Abstract

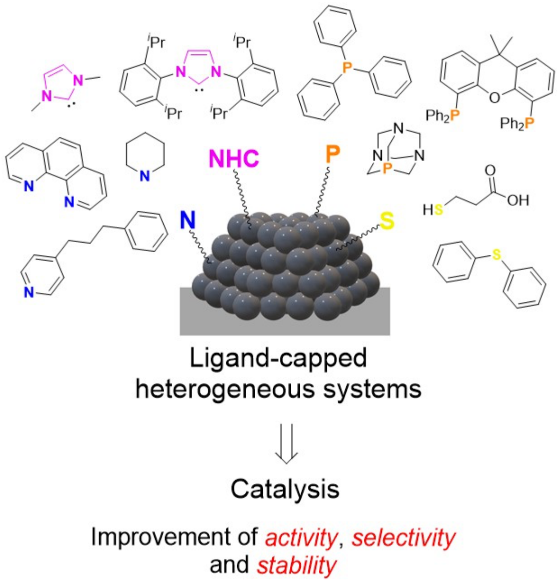

Abstract
This chapter focuses on the functionalization of heterogeneous catalysts of group 8-10 by capping ligands. The synthetic approaches used for the introduction of ligands were particularly looked at and according to the type of ligands, 3 main approaches were used: the colloidal formation of metal nanoparticles (MNPs) stabilized by ligands and their subsequent deposition over a solid support, the direct synthesis by colloidal formation of the ligand-capped active phase in the presence of the support and the ligand functionalization of a previously synthesized heterogeneous catalyst. Depending on the aim of the study and the catalytic application, one of the synthetic strategies was selected. The ligands were shown to have a range of effect on the catalytic performance of the catalyst by tuning the electronic properties of the metal(s), the steric hindrance at the metal surface or blocking some of the catalyst active sites. These modifications can therefore influence the activity, the selectivity and/or the stability of the materials and as such, ligand functionalization appears as a powerful method to fine tune the properties of heterogeneous catalysts.

Keywords Ligands, Nanoparticles, Heterogeneous catalysts, Phosphorus, Nitrogen, N-Heterocyclic carbenes, S-donor, catalytic performance.

Contents

1. **Introduction**

2. **N-donor ligand-capped heterogeneous catalysts**
    2.1 N-ligand capped heterogeneous catalysts formed by colloidal methods prior to their deposition over a solid support
        2.1.a Aliphatic N-donor ligands
        2.1.b Aromatic N-donor ligands
        2.1.c Mixture of amine and carboxylic acid as capping agents
    2.2 N-capped heterogeneous catalysts formed by colloidal methods in the presence of the solid support
        2.2.a Aliphatic N-donor ligands
        2.2.b Aromatic N-donor ligands
        2.2.c Mixture of amine and carboxylic acid as capping agents
    2.3 N-capped heterogeneous catalysts formed by classical methods followed by ligand functionalization

3. **Phosphorus donor ligand-capped heterogeneous catalysts**
    3.1 Colloidal synthesis of P-capped MNPs followed by deposition over a solid support
    3.2 Colloidal synthesis of P-capped MNPs in the presence of a solid support
    3.3 Functionalization of previously synthesized heterogeneous catalysts using P-donor ligands
    3.4 Functionalization of the support/solvent using P-donor ligands

4. **NHC ligand-capped heterogeneous catalysts**
    4.1 NHC-capped heterogeneous catalysts formed by colloidal synthesis followed by deposition onto a solid support
    4.2 NHC-capped heterogeneous catalysts formed by colloidal synthesis in the presence of a solid support
    4.3 Functionalization of previously synthesized heterogeneous catalysts using NHC ligands
    4.4 Functionalization of the support by NHC ligands prior to MNP formation

5. **S-donor ligand-capped heterogeneous catalysts**
    5.1 S-donor ligand-capped heterogeneous catalysts formed by colloidal synthesis followed by deposition onto a solid support
    5.2 Functionalization of previously synthesized heterogeneous catalysts using S-donor ligands

6. **Conclusions and perspectives**

1. Introduction

Over the last decades, the preparation of metal nanoparticles (MNPs) by colloidal strategies has become an efficient tool for the controlled synthesis of heterogeneous catalysts.[1,2,3] In this approach, the binding of organic ligands (also called capping agents) at the metallic surface enables the precise control of MNP size, shape and composition (*i.e.*, surface structure). However, the presence of such ligands was traditionally believed to induce the blockage of the catalytic active sites and therefore to negatively affect the catalyst activity and various strategies were reported to remove these ligands without altering the surface properties of the MNPs.

More recently, the beneficial roles of surface ligands in terms of activity or selectivity of nanocatalysts has been demonstrated.[4] Indeed, the presence of ligands on metal surfaces can induce steric effect between ligands and reactants, electron transfer through the metal−organic interface, etc…[5] These capping ligands can be introduced in different manners depending on the nature of the support and future application of the nanocatalysts. Indeed, when the fine control of the MNP size and composition are aimed for, the ligands can be used as unique stabilizers in colloidal synthesis prior to their deposition onto a solid support. However, when the metal-support interactions are strong enough, the decomposition of the metal precursor can be performed in the presence of both the support and the capping agents. Moreover, the effect of the capping agents can also be directly probed by functionalization of an heterogeneous catalysts previously synthesized under classical conditions (**Fig. 1**).

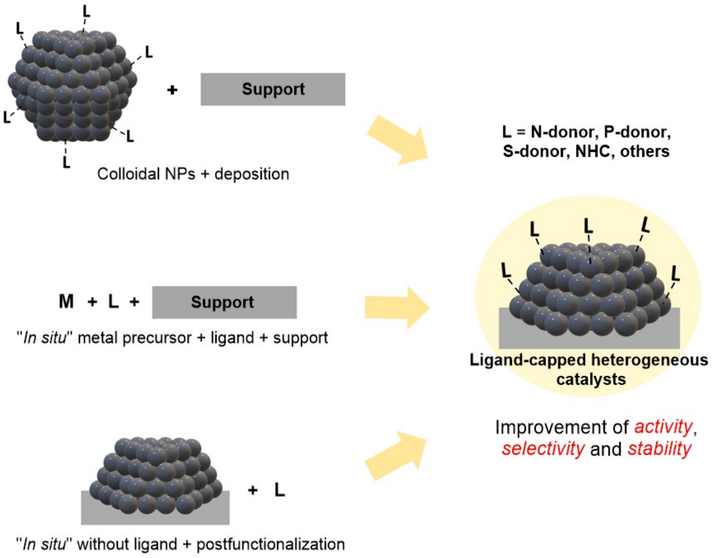

Fig. 1. Synthetic strategies for the formation of ligand-capped heterogeneous catalysts.

In this chapter, the effects of ligands on heterogeneous nanocatalysts are presented through literature examples and classified by the donor atoms of the ligands (**Fig. 2**) and the synthetic methodology utilized (**Fig. 1**). In view of the somewhat unclear definition of ligands in heterogeneous catalysis, the effects of capping agents described here will be limited to N-, P-, and S-donor molecules and NHC ligands. Recent results demonstrated that appropriate modifications of metallic nanoparticle-based catalysts by ligands can dramatically improve the activity/selectivity of specific catalytic reactions, mainly due to steric and electronic modifications of the heterogeneous nanocatalysts. The stability of ligand-promoted nanocatalysts before and after catalytic reactions is also discussed.

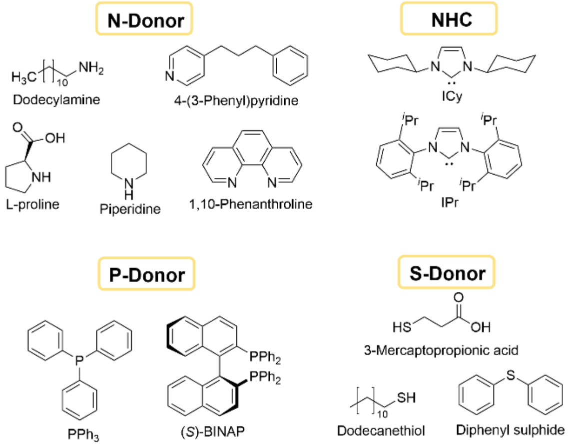

Fig. 2. Examples of ligands used to enhance the performances of heterogeneous catalysts.

2. N-donor ligand-capped heterogeneous catalysts

Generally, N-donor ligands were mainly utilized to finely tune the physical properties of the heterogeneous catalyst active phases through colloidal synthesis. Using this approach, the metallic active phases were formed in solution using N-based capping agents followed by their deposition over a solid support. This approach presents the advantage of precisely controlling the structure and composition of MNPs and to reach very high particle loadings. In colloidal chemistry, N-donor molecules were among the first ligands that were reported due to their ability to stabilize MNPs [6]. Since these early reports, a variety of N-donor ligands were used to improve the catalytic behavior of heterogeneous catalysts either during the synthesis of colloidal nanoparticles, during the formation of the nanoparticles in the presence of the support or by functionalization of the previously synthesized catalysts by addition of ligands.

The introduction of N-functions at the surface of the support during the catalyst synthesis has also attracted much interest [7]. In these cases, the N-based capping agents can be designed to either retain their structural properties or to be integrated within the solid support structure during a calcination step. Depending of the strategy to be used, either amines containing aliphatic chains or pyridine derivatives were reported as capping agents.

For instance, Guerrero, Rossi, Philippot and co-workers reported the preparation of palladium NPs supported over a magnetite-based support decorated by terpyridine ligands acting as stabilizers (**Fig. 3**) [8, 9]. The role of the terpyridine ligand was to control the size and stability of the palladium nanoparticles. Moreover, in hydrogenation reactions, the activity and selectivity of this nanocatalyst were enhanced compared to those provided by palladium nanoparticles supported on an amino-modified magnetic support.

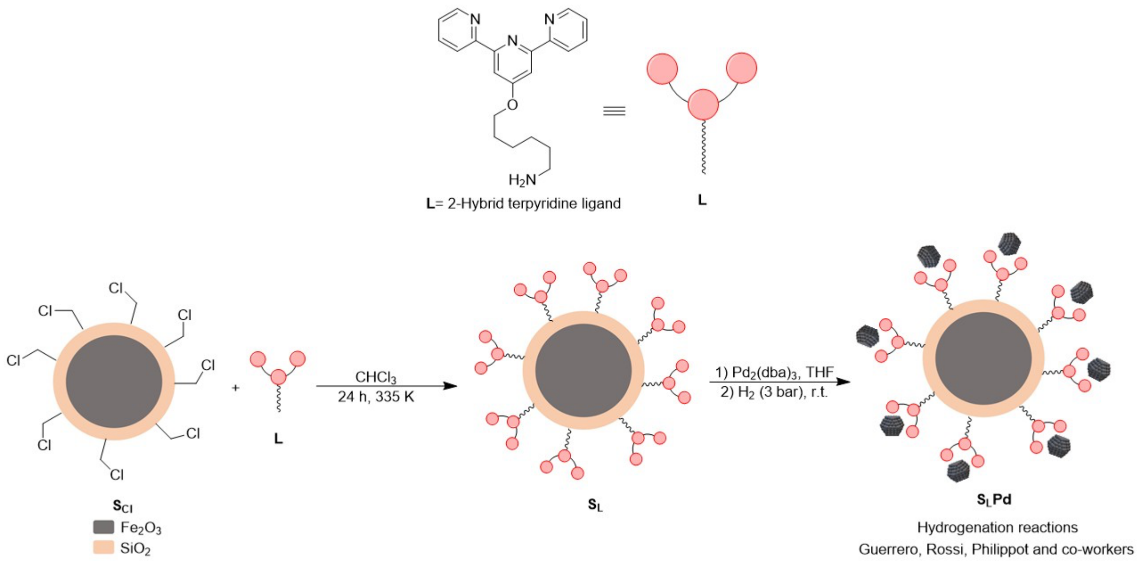

Fig. 3. Ligand modification of a support reported by Guerrero, Rossi, Philippot and co-workers.

Using a distinct approach, Chen and co-workers used ethylenediamine (EDA) as a nitrogen precursor for the synthesis of a Fe/Co-N_x composite onto nanoporous carbon black [10]. In this case, the N-donor ligands were used to stabilize the metal precursor prior to their decomposition upon heating the mixture. The resulting pyridinic-type nitrogen introduced in the catalysts revealed crucial for ORR catalytic activity and selectivity.

In the following sections, representative examples of heterogeneous catalysts containing N-donor ligands will be described and classified according to the synthetic approach used for the introduction of the N-donor ligands and its nature (i.e. aliphatic *vs* aromatic).

2.1-N-capped heterogeneous catalysts formed by colloidal methods prior to their deposition over a solid support

2.1.a Aliphatic N-donor ligands

Long chain aliphatic amines have been successfully used for the stabilization of well defined transition MNPs and their application in a range of applications.

For instance, in 2007, Nikles and co-workers prepared well-dispersed Pt NPs by polyalcohol reduction using oleylamine as capping agent that were subsequently loaded onto a carbon support for application in the electrocatalytic oxidation of methanol [11]. The ligand to metal ratio used in the synthesis affected the particle size and variations from 3.5 nm to 11.5 nm were observed when decreasing the amount of oleylamine. The as-prepared particles were subsequently deposited onto a carbon support but showed no electrocatalytic activity. An activation step involving the removal of the ligand from the surface of the Pt NPs was carried out by heating the particles in air at 185 ºC. Cyclic voltammetry showed that the ligand-free particles were electrocatalytically active for methanol oxidation. Interestingly, the smallest Pt NPs (3.5 - 4.0 nm) demonstrated a higher intrinsic activity for methanol oxidation, but a lower tolerance to CO poisoning, compared with the larger particles (6.0 - 11.5 nm).

In 2009, Peng and Yang described a new approach to address synergetic effects on both the activity and stability issues of electrocatalysts using palladium MNPs as support for Pt catalysts [12]. The Pt-on-Pd nanoparticles were prepared using a sequential synthetic method. The Pd NPs were formed by thermal decomposition of palladium acetylacetonate in the presence of oleylamine and trioctylphosphine and exhibited an average diameter of 5.3 ± 0.6 nm [13, 14]. The Pt NPs were formed by subsequent decomposition of Pt acetyl acetonate in the presence of the Pd NPs. The Pt NPs exhibited an average diameter of ~3 nm and were distributed evenly on the surface of Pd NPs. Similarly to the previous examples, activation was necessary and these bimetallic catalysts exhibited much higher activity and stability that the corresponding pure Pt catalyst, which was attributed to the favored interfacial structures between Pt and the Pd support.

Ramírez-Meneses and co-workers compared the performance of Pt NPs stabilized by different primary amines (i.e. tert-butylamine, 1,3-diaminopropane and anthranilic acid) in the oxygen reduction reaction (ORR) (**Fig. 4**). The MNPs were synthesized through the organometallic approach and subsequently supported over Vulcan carbon [15]. The resulting particle sizes ranged from 10 to 100 nm depending on the stabilizer. The catalytic results reveled an effect of the amine stabilizer and higher activities were obtained when the Pt NPs were capped by tert-butylamine.

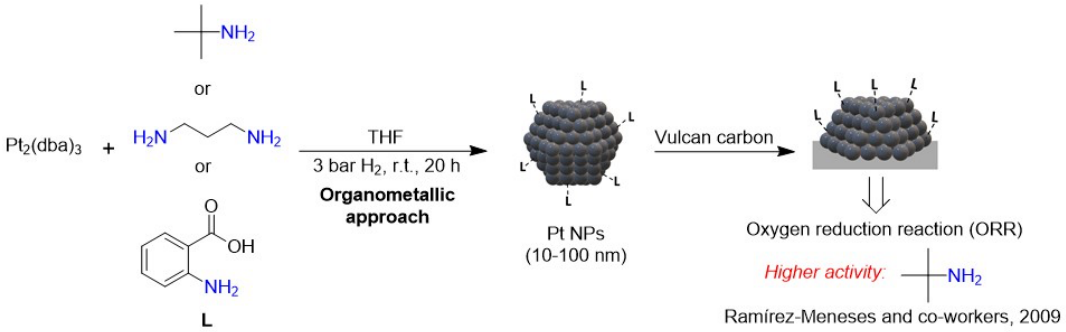

Fig. 4. Synthesis of N-capped Pt nanocatalysts reported by Ramírez-Meneses and co-workers.

More recently, Miyabayashi, Nishihara and Miyake reported the preparation of Pt NPs (2.4 - 2.8 nm) protected with octylamine (OA) and partly substituted by alkylamine with a pyrene group (PA) and supported over carbon black (i.e. Vulcan XC72) [16]. The synthesis of the ligand-stabilized MNPs was performed by chemical reduction with $NaBH_4$ [17]. The MNPs without any pretreatment to remove the introduced organic-protected agents were applied as catalysts for oxygen reduction reaction (ORR). The modification of the Pt NP surface with OA and PA considerably enhanced the electrocatalytic activity of the catalysts. Indeed, the area and mass specific activities increased at high PA/OA ratios. The potential cycle test demonstrates that the modification of Pt NPs by PA improves the stability of the catalyst and maintains high area and mass specific activities of ORR.

In 2017, Miyabayashi and Miyake reported the preparation of Pt NPs (2.6 nm) using undecafluorohexylamine (UFHA) and octylamine as stabilizing ligands and their subsequent deposition over acid-treated carbon black [10, 18]. The synthesis of Pt NPs using both ligands was performed following the modified two-phase liquid reduction method using $NaBH_4$ as reductant [16]. The carbon black supported systems were applied as electrocatalysts for the ORR. The affinity between the perfluorinated alkyl chains of UFHA and the Nafion® used as binder between the support and the catalyst improved the activity of the latter by generating a proton conduction path. Moreover, modification by UFHA enhanced robustness by avoiding Pt dissolution and carbon corrosion due to limited water accessibility.

In 2019, Ung and Cossairt prepared bare CoP nanocrystals that were decorated with carboxylates (i.e. oleate, octanoate, acetate) and amines (i.e. oleylamine, octylamine, dioctylamine, trioctylamine butylamine) and deposited over a carbon fiber electrode support with the aim of studying the effect of the ligand in catalysis [19]. Carboxylates and amines were selected as common stabilizers in colloidal syntheses and to evaluate the impact of their steric properties and hydrophobicity on catalysis. These systems were tested in the hydrogen evolution reaction (HER). Long chain carboxylates caused a larger increase in overpotential than their equivalent amines (e.g. oleate *vs* oleylamine), due to higher ligand density and stronger coordination of carboxylates. Moreover, carboxylates bearing longer carbon chain resulted in higher overpotential whereas no such an effect was observed with primary amines. These results suggested that the surface ligands hinder catalysis on CoP for HER mainly by preventing substrate access to surface active sites.

Wang, Lou and co-workers prepared novel 3D Pt nano assemblies consisting of 1D single-crystal Pt nanowires (diameter and length were in the range of 5–10 nm and 100–200 nm, respectively), by a one-pot method using oleylamine and cetyltrimethylammonium bromide (CTAB) as stabilizers [20]. In this case, oleylamine acted as solvent, reducing agent and stabilizer for the formation of metal nanostructures [21, 22]. Cetyltrimethylammonium bromide (CTAB) plays an important role as the structure-directing agent in the formation of multi-wire structures since only irregular multipods were obtained in the absence of CTAB [23]. When evaluated as electrocatalysts for low-temperature fuel cells, these interconnected 3D Pt nanostructures manifested high electrochemical surface area and significant long-term stability.

OA ligands were also used for thermocatalytic processes. For instance, Son and co-workers reported the synthesis of tetrahedral Rh nanoparticles (4.9 ± 0.4 nm) using oleylamine as stabilizing ligand that were subsequently loaded on charcoal [24]. Spherical Rh nanoparticles were also synthesized by hot injection method for comparison. Both catalysts were tested in the hydrogenation of arenes. The tetrahedral Rh NPs on charcoal provided much higher activity than the spherical nanoparticles and commercial Rh/C in the hydrogenation of anthracene. Moreover, the tetrahedral nanoparticles showed outstanding activity for a range of arenes.

Borchert and co-workers reported the preparation of Pt NPs and nanowires using dodecylamine (DDA) and/or hexanethiol as stabilizers for CO oxidation catalysis. These nano-objects were subsequently deposited over γ-alumina or silica [25]. CO adsorption experiments were performed for these systems and revealed that small molecules can pass through the ligand shell and adsorb on free areas of the Pt surface. These systems were active in the catalytic CO oxidation reaction. The differences in activity observed were ascribed to the morphology of the catalysts, nature of the support or differences in surface coverage by the ligand molecules. Interestingly, the Pt nanowires were restructured upon catalytic conditions and the shape of the Pt species in the spent catalyst was quasi-spherical.

Bäumer and co-workers reported a distinct approach based on the initial synthesis of colloidal ligand-free Pt NPs (2.2 ± 0.3 nm) by metal salt reduction in ethylene glycol (EG) and the subsequent functionalization with DDA (2.2 ± 0.3 nm) [26]. Then, the coating of three different monolithic supports (i.e. cordierite honeycomb, Al_2O_3 foam and Nickel fleece) was performed with preformed ligand-free and ligand-stabilized Pt NPs. Interestingly, prior to the deposition of the MNPs the supports were functionalized with the ligands. The formation of this ligand double layer was shown to avoid the formation of an alloy between the MNP and the support and as such, high activity for CO oxidation was maintained. In contrast, when no ligand was used, the catalytic activity decreased over time. Similarly, the same authors later reported the deposition of ligand-free (2.3 ± 0.2 nm), dodecylamine-capped (2.3 ± 0.2 nm) or dodecanethiol (DDT) Pt NPs supported over Fe_3O_4 and showed that the presence of ligands at the Pt surface avoids unfavorable strong metal–support interactions (SMSI) and as such, enhance the activity of the catalysts in CO oxidation [27]. They also reported the deposition of ligand-free and dodecylamine-capped Pt NPs (1.9 - 2.2 nm) over three different support materials with varying acid/base properties, namely γ-Al_2O_3, SiO_2 and MgO [28]. The nanoparticles were prepared in ethylenglycol (EG) and subsequent functionalization with DDA was performed using a phase-transfer method [29, 30] (**Fig. 5**).

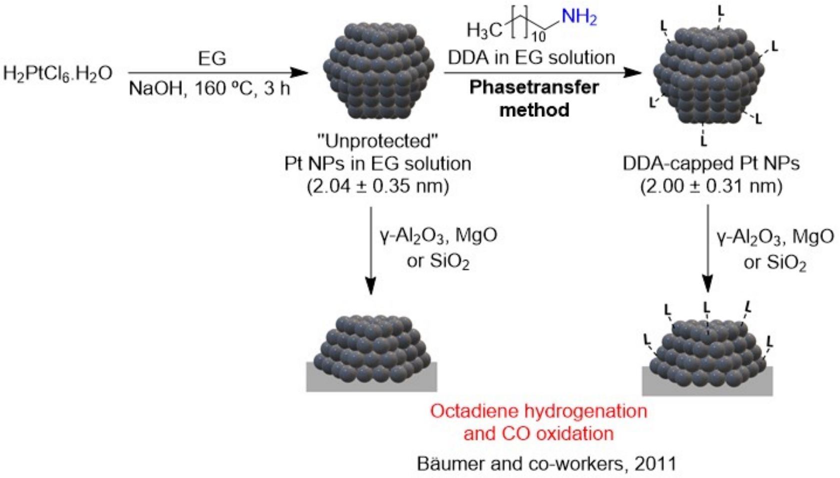

Fig. 5. Preparation of Pt catalysts by Bäumer and co-workers.

This constituted the first systematic study on the influence of ligands in heterogeneous gas-phase catalysis using identical nanoparticles synthesized by colloidal methods. The catalytic properties of these catalysts were investigated in two reactions. First, octadiene hydrogenation was used as a test reaction to probe the influence of the ligands under reducing conditions temperatures ($T < 100$ ºC). The ligands strongly modified the metal–support interactions and exerted a protecting effect with respect to support induced oxidation during the deposition step. When SiO_2 was the support, where surface oxidation is more prominent, the ligand-capped catalyst was significantly more active than the ligand-free analog. When the catalysts were tested in CO oxidation at high temperatures ($T \approx 200$ ºC), decomposition, desorption and spillover of ligands on the support became important. Depending on the supports, the ligand coverage varied and spillover was most evident on Lewis acidic γ-Al_2O_3 compared to the Brønsted acidic SiO_2.

In 2013, Altmann, Bäumer and co-workers reported the preparation of colloidal ligand-capped (i.e. DDA) Pt (2.2 ± 0.3 nm) and bimetallic PtSn (2.3 - 2.4 nm) nanoparticles that were subsequently deposited on SiO_2 for the selective semi-hydrogenation of acetylene in ethylene-rich streams [31]. To assess the effect of ligands on catalysis, monometallic and bimetallic DDA-capped MNPs were compared with ligand-free catalysts. Both surface ligands and Sn enhance the selectivity and the most selective catalyst was the DDA-capped PtSn catalyst (metal atom ratio of 1:1).

Philippot, Rossi and co-workers reported the preparation of bimetallic NiPd nanoparticles (5-6 nm) via the organometallic approach using hexadecylamine (HDA) as stabilizing ligand and supported over magnetic silica [32]. Nickel−palladium nanoparticles were supported onto a magnetic silica using various Ni/Pd ratios. The supported catalysts were evaluated in the hydrogenation of cyclohexene and their performance compared to the corresponding monometallic catalysts. The catalysts prepared using a 1:9 Ni/Pd molar ratio provided the highest initial activity (i.e. > 50 000 h^{-1}), greater than the monometallic Pd catalyst. Moreover, excellent separation from the products could be performed without metal leaching, leading to an efficient recycling.

More recently, Domingos, Philippot and co-workers reported the preparation of a series of Ni(0) nanocatalysts prepared through the organometallic approach in the presence of hexadecylamine (HAD), polyvinylpyrrolidone (PVP), PVP/triphenylphosphine, octanoic acid (OA) and stearic acid. The resulting MNPs exhibited diameters of *ca*. 5-6 ± 2nm and were evaluated in the selective hydrogenation of α,β-unsaturated carbonyl compounds by H_2 under mild reaction conditions [33]. The system in which OA was used as ligand was also deposited over SiO_2. All catalysts were active in the chemoselective hydrogenation of the C=C bond, which was attributed to the reduced nature of the Ni NPs surface. Moreover, the hydrogenation reaction rate revealed sensitive to the stabilizer type, with the carboxylic acid-stabilized systems providing the best performances. Moreover, the supported catalyst could be reused up to 10 times without significant loss of activity.

Pérez-Yuste and co-workers presented a novel strategy based on the immobilization of oleylamine-stabilized Pd NPs (3.0 ± 0.4 nm) on filter paper for development of a catalytic system with high efficiency and recyclability [34, 35]. The final material was prepared by a simple dip-coating process using highly concentrated MNP dispersions in volatile organic solvents and tested in several model reactions such as the oxidative homocoupling of arylboronic acids, the Suzuki cross-coupling reaction, and nitro to amine reduction. These N-capped heterogeneous catalysts displayed efficient catalytic activity and excellent recyclability and reusability.

The same year, Kunz and co-workers reported the preparation of well-defined DDA-capped bimetallic PtSn nanoparticles (*ca*. 2 nm) by colloidal methods that were subsequently deposited on TiO_2 (**Fig. 6**) [36]. The influence of the Pt/Sn ratio on the catalytic properties for the hydrogenation of crotonaldehyde was looked at. The activity of Pt increased significantly by adding small amounts of Sn (10%), which was attributed to an electronic effect. However, a gradual decrease was observed when the Sn content was further increased, which attributed to the loss of Pt sites needed for the activation of H_2. The lower activity was accompanied by a constant selectivity increase towards crotylalcohol. In this study, activity and selectivity followed clear trends related to the

Sn content, which emphasizes the potential of colloidal chemistry for model studies in heterogeneous catalysis.

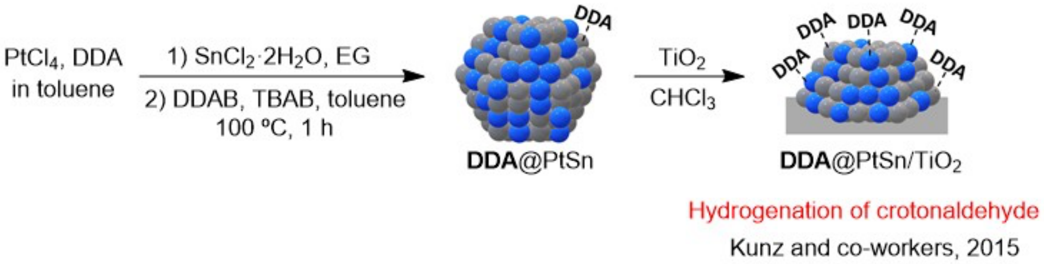

Fig. 6. Preparation of well-defined amine-capped bimetallic PtSn nanoparticles and their subsequent deposition on TiO_2.

More recently, Fan and co-workers used a slightly distinct approach for the synthesis of rhodium nanoparticles bearing L-proline as capping agent [37]. The preparation was performed by chemical reduction of $RhCl_3$ with $NaBH_4$ in the presence of L-proline and without isolation, the MNPs were then deposited on carbon (**Fig. 7**). In this synthesis, L-proline was employed as a size controller for the synthesis of small (~2 nm) and uniform Rh NPs for the first time.

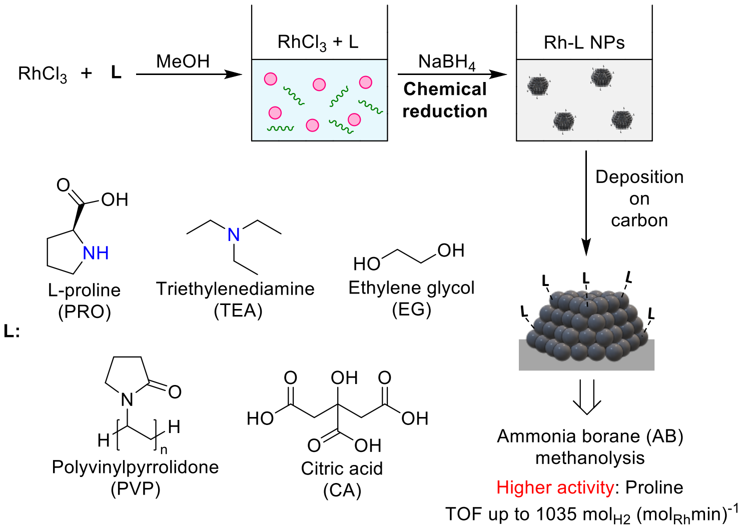

Fig. 7. Ligand-stabilized Rh NPs supported on carbon reported by Fan and co-workers.

The Rh catalysts showed high activity for ammonia borane (AB) methanolysis with a total turnover frequency (TOF) up to 1035 mol_{H_2} $(mol_{Rh}min)^{-1}$ under basic conditions. This excellent catalytic performance was attributed to the well-dispersed Rh NPs and the functionalized metal surface, which provided more active sites for the reaction. Other ligands such as ethylenediamine, triethylamine, ethylene glycol, polyvinylpyrrolidone and citric acid were used for the preparation of analogous catalysts, however, the best results were obtained with the L-proline-functionalized Rh catalyst.

2.1b Aromatic N-donor ligands

Aromatic N-based donor molecules were also used for the preparation of N-ligand-capped heterogeneous catalysts.

For instance, in 1993, Schmid and co-workers reported the deposition of Pd clusters (between 31.5 and 36.0 Å) stabilized with phenanthroline over TiO_2 [38]. The resulting material was used as catalyst in the semi-hydrogenation of alkynes with selectivity to the corresponding alkene up to 98%. In 1996, Schmid and co-workers reported the use of ligand-stabilized palladium clusters (3-4 nm) on various supports such as TiO_2, Al_2O_3 and $CaCO_3$ for applications in gas phase and liquid phase hydrogenation and semi-hydrogenation reactions [39, 40]. For example, N-donor ligands such as di-2,9-(2-methyl-butyl)-1,10-phenanthroline and (-)-cinchonidine were employed in the catalytic semi-hydrogenation of 2-hexyne. The phenanthroline stabilizer improved the selectivity of the reaction by suppressing isomerization and over hydrogenation reactions. In the hydrogenation of acetophenone, the stabilizers mainly affected the activity of the catalysts.

In 1997, Schmid and co-workers reported the preparation of p-$H_2NC_6H_4SO_3Na$ (sodium sulfanilate)-stabilized Pt shell on Au or Pd cores supported onto alumina and TiO_2 for their application in hydrosilylation reactions [41, 42, 43]. The aim of these works was to study the influence of the electronegativity of the colloidal core metals on the activity and selectivity of the Pt surface in hydrosilylation reactions.

Gómez and co-workers reported the synthesis of small and well-dispersed Ru NPs stabilized by 4-(3-phenylpropyl)pyridine as ligand and supported over different supports, such as Al_2O_3, SiO_2, activated carbon (AC) and multi-walled carbon nanotubes (MWCNT) [44]. The synthesis of the catalyst was carried out in two steps: first, the preparation of colloidal MNPs (1.3 ± 0.4 nm, **Fig. 8**) [45] and their subsequent immobilization over the corresponding support.

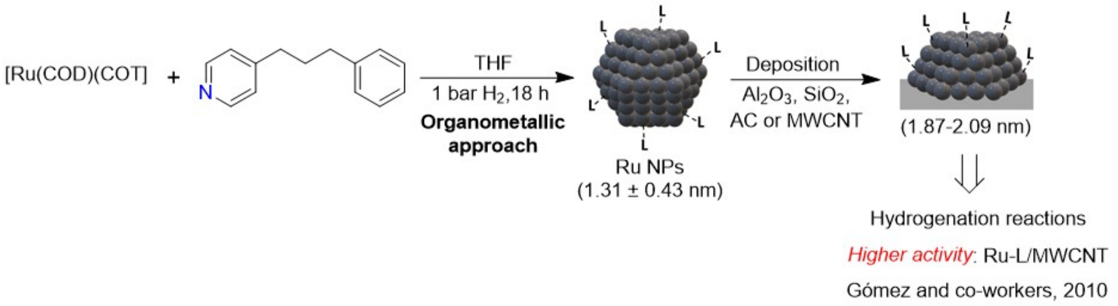

Fig. 8. Ru NPs stabilized by 4-(3-phenylpropyl)pyridine and supported over different supports, including MWCNT.

These supported catalysts were used in the hydrogenation of several unsaturated substrates. The effect of the supports was particularly looked at and the highest activity, chemoselectivity and recyclability was observed for the Ru-L system immobilized over MWCNT.

In 2011, the same group reported the preparation of well-dispersed Pd NPs in ionic liquids in the presence of 4-(3-phenylpropyl)pyridine and their subsequent immobilization onto multiwalled carbon nanotubes (MWCNTs) modified with imidazolium moieties [46]. When the synthesis of the MNPs was performed in the presence of the ligand in [BMI][PF_6] as solvent, the obtained MNPs exhibited a size of 4.5 ± 0.8 nm. In the absence of the ligand, the particle size was similar (4.5 ± 1.0 nm) but a more heterogeneous dispersion was observed. Once dispersed over the support, this catalyst was tested in hydrogenation and Heck coupling reactions and could be recycled up to four times without significant activity loss.

Recently, García-Antón, Sala and co-workers reported the synthesis of a hybrid material ($Ru@RuO_2PPTiO_2$-RuP) based on 4-phenylpyridine-capped Ru nanoparticles (RuPP), TiO_2 nanocrystals and $[Ru(bpy)_2(4,4'-(PO_3H_2)_2(bpy))]Cl_2$ (RuP) as catalyst for the hydrogen evolution reaction (HER) [47]. The preparation of this catalyst was performed in three steps. First, the Ru NPs (1.4 ± 0.3 nm) capped with 4-phenylpyridine were prepared though the organometallic approach [48] followed by their deposition onto TiO_2 by impregnation (1.7 ± 0.4 nm), and the decoration of the latter with a visible-light photoabsorber (RuP). TiO_2 acted as an efficient dispersing agent and stabilizer for the catalyst ($Ru@RuO_2PP$) and electron relay between $Ru@RuO_2PP$ and the photoabsorber (RuP) under irradiation. Thus, this double role of TiO_2 as support and electron-mediator enabled the first efficient visible-light-driven HER photocatalysis based on a Ru-based photocatalyst and a molecular photoabsorber.

In the area of asymmetric catalysis, Bönnemann and Braun reported in 1997 the first example of MNPs stabilized by chiral molecules as a new type of enantioselective heterogeneous catalysts, combining good selectivity control and high activity in asymmetric hydrogenation reactions [49]. In their work, colloidal Pt NPs were stabilized by the alkaloid dihydrocinchonidine and subsequently supported over silica. Both colloidal and supported systems exhibited the same MNP size. These systems were tested in catalysis and compared with a commercial heterogeneous catalyst. The colloidal systems provided higher conversions and enantiomeric excess (*ee*) values than the two supported heterogeneous catalysts.

2.1c Mixture of amine and carboxylic acid as capping agents

In 2010, Yang and co-workers reported the synthesis of Pt_3Ni catalysts with using long-chain amines as capping agent and Vulcan carbon as support [50]. In this system, adamantanecarboxylic acid (ACA) or adamantaneacetic acid (AAA) were also employed [51]. At a later stage, butylamine was used to replace the capping agents used during the synthesis of Pt_3Ni nanocrystals and to generate carbon-supported active electrocatalysts that exhibited enhanced activity compared to commercial catalysts.

In 2012, Yang and co-workers described the synthesis of PtM (M = Au, Ni, Pd) (PtAu particle size: 11 ± 0.2 nm; Pt_3Ni particle size: 13 ± 0.3 nm) icosahedral nanocrystals [52]. The synthesis was performed using the gas reducing agent in liquid solution (GRAILS) method [53], which requires the use of carbon monoxide (CO) [54]. In this study, oleylamine (OAm) and oleic acid (OA) were used in the synthetic mixture and the resulting MNPs were supported over carbon. Both CO gas and organic surface capping agents play critical roles in stabilizing the icosahedral shape with {111} surfaces. Among the PtM alloy nanocrystals, Pt_3Ni revealed very active with an impressive ORR specific activity of 1.83 mA/cm^2 Pt and 0.62 A/mg_{Pt}.

In 2012, Strasser and co-workers reported the preparation of a series of dealloyed Pt_xNi_{1-x} core–shell nanoparticles [55] in the presence of oleic acid (OAc), oleylamine (OAm) and 1,2-tetradecandiol (TDD), which were subsequently supported over carbon. The particle size of the PtNi, $PtNi_3$, and $PtNi_5$ NPs were 5.1 ± 0.6, 8.3 ± 0.8, and 12.1 ± 1.1 nm, respectively. The radial location and the composition of the Ni-enriched inner shells were dependent on the initial alloy compositions. These self-organized Ni enriched inner shells revealed to play a key role in maintaining surface lattice strain and thus control the surface catalytic activity in the oxygen reduction reaction (ORR).

Bäumer and co-workers also prepared colloidal PtNi nanoparticles (~ 4 nm) using OAm and OA as organic stabilizers [56], and their deposition onto γ-Al_2O_3 and MgO powders [57]. These materials were tested in the CO oxidation reaction and no pre-treatment was needed to obtain immediate activity. The results prove that well-defined catalysts with exceptional activities can be obtained with this approach and the authors concluded that the residual ligands could have a protecting effect.

In 2014, Yin, Ma and co-workers reported for the first time the preparation of monodispersed bimetallic PdAg NPs using OAm and OA as capping agents and carbon black as support [58]. The bimetallic PdAg NPs were synthesized via the thermal decomposition of palladium acetate and reduction of silver acetate in the emulsion-assisted ethylene glycol ternary system [59]. Various compositions of bimetallic PdAg nanoparticles, $Pd_{80}Ag_{20}$ (3.8 nm), $Pd_{65}Ag_{35}$ (3.6 nm) and $Pd_{46}Ag_{54}$ (3.3 nm) were obtained by modifying the reaction parameters. The PdAg systems were supported on carbon black without any post-treatment and provided high electro-oxidation activity towards methanol oxidation in alkaline media. The carbon-supported $Pd_{80}Ag_{20}$ nanoparticles revealed superior activity than that of the commercial Pt/C electro-catalyst. It was concluded that the enhanced activity was dependent on the unique twinning structure of the catalyst.

In 2009, Rinaldi, Zanchet and co-workers reported the preparation of colloidal Ni NPs (5.3 nm) stabilized by trioctylamine and OA and their deposition over silica and activated carbon. Subsequently, trioctylphosphine was added [60, 61, 62]. These heterogeneous catalysts were applied in the hydrogenation of cyclohexene and the steam reforming of ethanol [63]. The impregnation onto silica resulted in high metal dispersion. However, no or low catalytic activity was observed. The detailed surface analysis of the Ni/SiO_2 sample showed that the capping-ligands are not easily removed from the Ni surface in the posterior steps of the catalyst preparation, inhibiting the surface activation of the reactants.

In 2022, Serp, Soulantica and co-workers reported the synthesis of freestanding and few-layer graphene (FLG)-supported ε-Co nanoparticles and hexagonal closepacked hcp-Co nanorods stabilized by lauric acid (LA) and hexadecylamine (HDA) [64]. Cobalt nanostructures were synthesized by the reduction of $[Co\{N(SiMe_3)_2\}_2(thf)]$ by H_2 in the presence of LA and HDA [65, 66]. The authors showed that while hcp-Co nanorods exposing a majority of $\{11\bar{2}0\}$-type facets are the most active in the selective hydrogenation of cinnamaldehyde to cinnamyl alcohol, the supported spherical ε-Co nanoparticles combined high activity and excellent selectivity. The concentration-dependent ligand conformation on the surface of the nanostructures also influences their catalytic performances, as higher concentrations favored both activity and selectivity to cinnamyl alcohol.

In 2010, Sun and co-workers described the preparation of monodisperse Ni NPs by $Ni(acac)_2$ reduction using borane tributylamine (BTB) in the presence of OAm and OA. The Ni NPs dispersed on Ketjen carbon were highly active for hydrolytic dehydrogenation of the ammonia-borane (AB) complex at room temperature [67]. In this process, OAm acted as both solvent and surfactant, BTB was the reducing agent, and OA was added as cosurfactant for Ni NP stabilization.

2.2 N-capped heterogeneous catalysts formed by colloidal methods in the presence of the solid support

Another approach for the synthesis of N-donor ligand-capped heterogeneous catalysis is the direct reduction of the metal precursor in the presence of both the support and the stabilizing ligands. In this approach both the support and the ligands participate in the stabilization of the MNPs.

2.2a Aliphatic N-donor ligands

Jang and co-workers reported the synthesis of Pt NPs supported over carbon using OAm as ligand for their application as electrocatalysts in proton exchange fuel cells [68]. For the preparation of this material, a mixture of the metal precursor, OAm, carbon black and $NaBH_4$ as reducing agent, was used with to produce MNPs with diameters between 2 and 3 nm. The performance of this catalyst was compared with that of a commercial Pt/C modified by OAm. The electrocatalyst prepared by the authors showed higher ORR activity and kinetic current density. They concluded that the surface ligands selectively blocked large anion adsorption and as such enhanced the catalytic activity since small oxygen molecules can still adsorb and react.

In 2020, Serp, Soulantica and co-workers reported the preparation of octadecylamine (ODA)-stabilized platinum concave nanocubes supported on graphene exposing {110} facets using an *in-situ* process and their subsequent use as catalysts in the selective hydrogenation of cinnamaldehyde [69]. The nanocubes were directly grown onto the a FLG support in the presence of ODA as stabilizing agent. Two sets of unsupported nanocubes stabilized by ODA were also prepared following literature procedures for comparison purposes [70]. Immobilization improved both activity and selectivity towards the desired unsaturated alcohol. The FLG-supported concave nanocubes presented outstanding activity and selectivity to cinnamyl alcohol higher than 80%. The presence of the organic stabilizer ensured the stability of the nanoparticle morphology and influenced the catalyst performance. While higher activity was obtained using small nanoparticles and low ligand contents, the selectivity to the unsaturated alcohol was favored by high ligand contents, probably due to steric effects favoring the substrate adsorption through the C=O moiety. Apart from stabilizing the nanocubes, the authors reported the presence of interactions between the support and the long chain amine ligand, and as such behaved as a ligand reservoir.

2.2b Aromatic N-donor ligands

In 2010, Esteruelas and co-workers reported the synthesis of Rh NPs (1.5 ± 0.2 nm) by decomposition of the pre-synthesized chloro[2,6-bis{1-(phenyl)iminoethyl}pyridine]rhodium(I) complexes [71]. The obtained Rh NPs were stabilized by the partially hydrogenated ligand. The nanoparticles were also generated in the presence of alumina as support. Under a constant atmospheric pressure of hydrogen, the nanoparticles catalyzed the dehalogenation and the hydrogenation of different substrates. However, Hg(0) poisoning test revealed that both homogeneous and heterogeneous catalysts coexist during the dehalogenation reactions whereas the hydrogenation processes were only catalyzed by heterogeneous catalysts.

In 2017, Hayashi and co-workers reported the preparation of nickel nanoparticles (*ca*. 4 nm) stabilized with pyridine ligands and supported over ZSM-5 zeolite [72]. The synthesis of the catalyst was carried out by $NaBH_4$ chemical reduction of the metal precursor in the presence of pyridine and the ZSM-5 zeolite support. Pyridine played a crucial role in the selective formation of small and well dispersed Ni NPs and increased their stability by enhancing the interaction between the Ni and the support. This catalyst provided the first complete hydrogenation of phenolic compounds as lignin monomers with higher activity than that of conventional Ni catalysts. Upon recycling, no relevant increase in size was observed after each catalytic cycle when pyridine was used in the synthesis of the MNPs whereas a large increase in diameter was evidenced for those synthesized in the absence of pyridine.

In 2009, Serp and co-workers reported the preparation of PtRu NPs (*ca*. 2 nm) stabilized by 4-(3-phenylpropyl) pyridine ligand containing a pyridine unit that has an affinity for the surface of the MNPs and a phenyl group able to interact with the carbon nanotube (CNT) graphene layers (π–π interaction) [73]. The authors also functionalized the CNT external surface with carboxylic acid and amide groups bearing a long alkyl chain to induce weak interaction or repulsion between the MNPs and the CNT external surface. These nanocatalysts displayed excellent catalytic performance in the selective hydrogenation of cinnamaldehyde owing to confinement of both the active phase and the reactants in the inner cavity of the CNTs.

2.2c Mixture of N-donor and carboxylic acid

Serp, Soulantica and co-workers reported the preparation of non-promoted Co/Al_2O_3–SiO_2 catalyst for Fischer–Tropsch synthesis (FTS) using hexadecylamine (HDA) and lauric acid (LA) ligands as MNP stabilizers [74]. Cobalt nanorods were prepared by growing anisotopic hcp-cobalt nanostructures on conventional Co/Al_2O_3–SiO_2 catalyst through the so-called seeded growth method [75]. The as-obtained catalyst showed a better stability than a reference catalyst for FTS. The removal of most of the ligands from the nanorod further enhanced the catalyst activity while maintaining its stability [76]. Previously, the same group reported monolithic *hcp*-cobalt nanowires bearing HDA and LA as ligands and supported over copper and nickel foams through a wet chemistry approach [77, 78, 79]. The Co/Cu_{foam} catalyst was tested in the Fischer–Tropsch synthesis in a fixed-bed reactor, providing superior activity and selectivity towards C_{5+} than a Co/SiO_2-Al_2O_3 reference catalyst. In this work, a negative effect of the ligands was described [74].

2.3 N-capped heterogeneous catalysts formed by classical methods followed by ligand functionalization

Other N-capped heterogeneous catalysts only involve the functionalization of the metal surface by the N-ligand in a final step of the synthesis. Usually, the capping of heterogeneous catalyst by N-donor molecules was performed to tune the selectivity of the catalytic reactions.

In an early example, Vasudevan and co-workers reported the effect of piperidine addition over Pd NPs supported on Al_2O_3 prepared by wet impregnation for the hydrogenation of unsaturated hydrocarbons [80, 81, 82]. The addition of piperidine during catalysis improved the hydrogenation rate and the selectivity, which was attributed to the electron donating properties of the piperidine ligands that decreased the bonding energy of the hydrocarbons.

In 2013, Sung and co-workers reported the modification of Pt/C (~ 5 nm) with oleylamine to prepare a carbon-supported platinum electrocatalyst for oxygen reduction reaction (ORR) [83]. The addition of a small amount of OAm on Pt NPs resulted a significant enhancement of the catalyst activity, which was attributed to both the downshift of the frontier d-band structure of platinum and the hindering of anionic spectator species that leads to an enhancement of ORR kinetics. These results suggest that the use of capping organic molecules could be a strategy to design advanced electrocatalysts via the alteration of both structural and electronic properties.

More recently, Chen and Xu immobilized some ligands containing secondary or tertiary amine groups and hydrophobic chains (**Fig. 9**) onto TiO_2-supported Ru nanoparticles [29]. The immobilization of the ligands onto Ru/TiO_2 was based on a simple two-phase centrifugation technique and driven by the hydrophobic effect. Additionally, the synthesis of ''unprotected'' Ru NPs (2.5 nm) was carried out according to previously reported methods [84] and subsequently immobilized onto TiO_2 by sol immobilization (2.0 nm) [85].

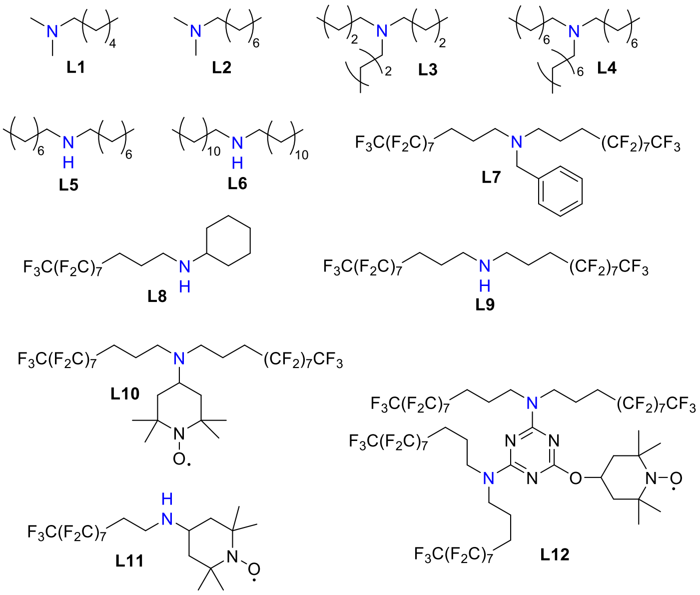

Fig. 9. Amine ligands used by Chen and Xu to functionalize TiO_2 supported Ru NPs.

These systems were tested in the aerobic oxidation of alcohols and ligands containing 2,2,6,6-tetramethyl-1-piperidine-Noxyl (TEMPO) moieties (L10, L11 and L12) significantly improved the selectivity to the aldehyde at high conversions.

Later, the same authors reported the modification of Pt/SiAl catalyst with ethylenediamine (EDA) by co-impregnation method and its application in the selective catalytic oxidation of ammonia [86]. TEM measurements demonstrated that the average particle sizes of Pt species decreased from 2.8 nm to 2.0 nm upon diamine addition. The results based on precise characterization indicated that the addition of EDA could adjust the states and particle sizes of Pt, and the reduction property of Pt/SiAl catalyst.

The functionalization of heterogeneous catalysts by chiral N-donor amines was also reported. Indeed, the first examples of asymmetric hydrogenations catalyzed by metal surface modified by the presence of (*S*)-proline (and other chiral molecules) as additive under catalytic conditions were first reported in the 1980’s by Petró and co-workers [87, 88, 89]. This strategy was used to induce enantioselectivity in the asymmetric hydrogenation of α,β-unsaturated ketones.

More recently, Liu, Shen and co-workers reported the use of a series of Pd/MgO catalysts modified by (*S*)-proline for the hydrogenation of isophorone (**Fig. 10**) [90]. The Pd/MgO catalysts were synthesized by the impregnation method and variations in MNP size were observed depending on the temperatures employed during calcination and hydrogen reduction. Particles sizes between 1 and 25 nm were obtained. In this study, it was demonstrated that Pd surfaces not only supply chemisorbed hydrogen but also participate in the enantio-differentiating step. Indeed, the configuration of the chiral product could be tuned by varying the size of Pd NP. In this process, two competitive reactions were identified: the formation of excess (*R*)-TMCH enantiomer was reached through the enantioselective hydrogenation of intermediates formed between isophorone and (*S*)-proline on Pd particles with a mean diameter >10 nm , while the direct hydrogenation of isophorone yielded racemic TMCH over Pd particles smaller than 4 nm, followed by kinetic resolution that yielded the (*S*)-TMCH enantiomer in excess.

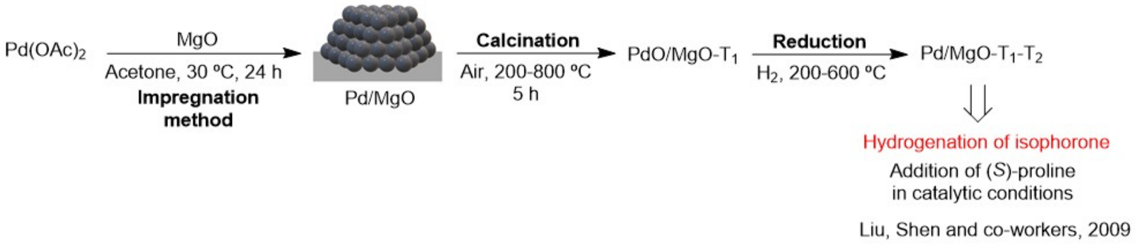

Liu, Shen and co-workers, 2009

Fig. 10. Preparation of Pd/MgO catalysts modified by (*S*)-proline for the hydrogenation of isophorone.

In 2010, Győffry and co-workers also reported the use of Pd NPs supported over various supports for the kinetic resolution of 3,5,5-trimethyl cyclohexanone (TMCH) and asymmetric hydrogenation of isophorone (3,5,5-trimethyl cyclohex-2-enone) in the presence of (*S*)-proline [91].

Aromatic N-donor ligands were also used as metal surface capping agents. In an early example, Baiker and co-workers reported the modification of commercial Pt/Al_2O_3 with cinchonidine as additive for the asymmetric hydrogenation of activated ketones such as ketopantolactone and ethyl pyruvate [92]. The catalytic reactions were carried out in a fixed-bed reactor with continuous feeding of the chiral modifier into the reactant stream. Total chemoselectivity was obtained with enantiomeric excesses of 83.4% for ketopantolactone, and 89.9% *ee* for ethyl pyruvate.

Blaser and co-workers also reported the use of commercial Pt/Al_2O_3 for the asymmetric hydrogenation of ethyl pyruvate using chiral modifiers derived from natural cinchona alkaloids [93]. Effects related to the structure of the chiral modifiers were studied. The strongest effects on *ee* were observed for changes in the $O\text{-}C_9\text{-}C_8\text{-}N$ part of the cinchona alkaloid and for partial or total hydrogenation of the quinoline rings (**Fig. 11**).

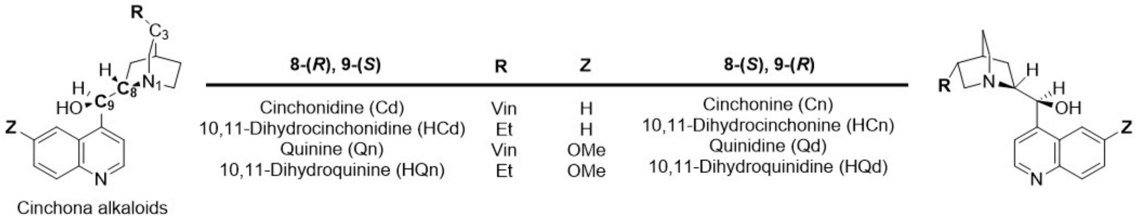

8-(*R*), 9-(*S*)	R	Z	8-(*S*), 9-(*R*)
Cinchonidine (Cd)	Vin	H	Cinchonine (Cn)
10,11-Dihydrocinchonidine (HCd)	Et	H	10,11-Dihydrocinchonine (HCn)
Quinine (Qn)	Vin	OMe	Quinidine (Qd)
10,11-Dihydroquinine (HQn)	Et	OMe	10,11-Dihydroquinidine (HQd)

Fig. 11. Chiral modifiers derived from cinchona alkaloids used for the modification of Pt/Al_2O_3 catalysts for application in asymmetric hydrogenation of ethyl pyruvate.

The solvent also demonstrated to have a significant effect on enantioselectivity and reaction rate and it was concluded that an efficient modifier for the hydrogenation of R-keto esters must contain a basic nitrogen center close to stereogenic center(s) and connected to an aromatic system.

Similarly, the modification of Pt NPs (4.4 nm) immobilized over silica coated Fe_3O_4 by cinchonidine was reported for the enantioselective hydrogenation of activated ketones (**Fig. 12**) [94]._The catalyst could be recycled up to eight times with little variation in activity although the enantioselectivity slightly decreased from 57% to 52% *ee* after the eighth cycle.

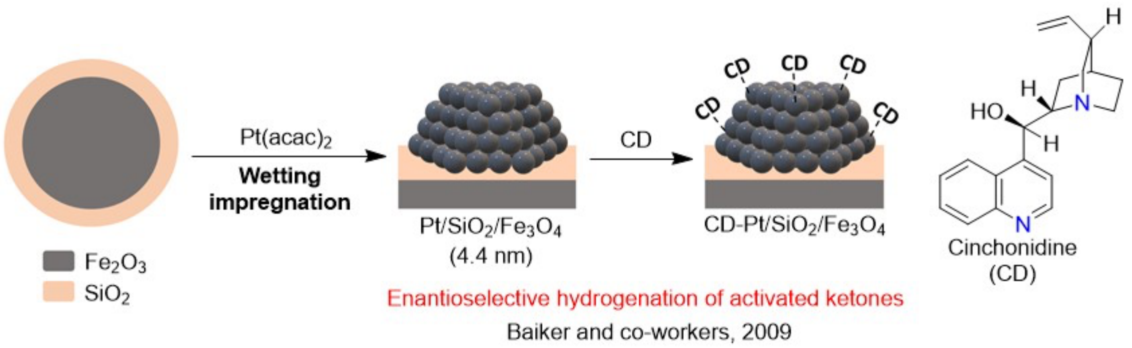

Enantioselective hydrogenation of activated ketones

Baiker and co-workers, 2009

Fig. 12. Modification of Pt catalysts on silica coated Fe_3O_4 by cinchonidine.

In 2010, Sugimura and Ogawa reported the use of cinchonidine (CD) and cinchonine (CN) as chiral modifiers for Pd/C in enantioselective hydrogenation reactions (**Fig. 13**) [95]. The catalytic hydrogenation with CD always provided higher *ee* and faster reaction rate than that with CN and it was concluded that the difference between CD and CN was not in their adsorption properties, but in the enantioinduction ability of these modifiers.

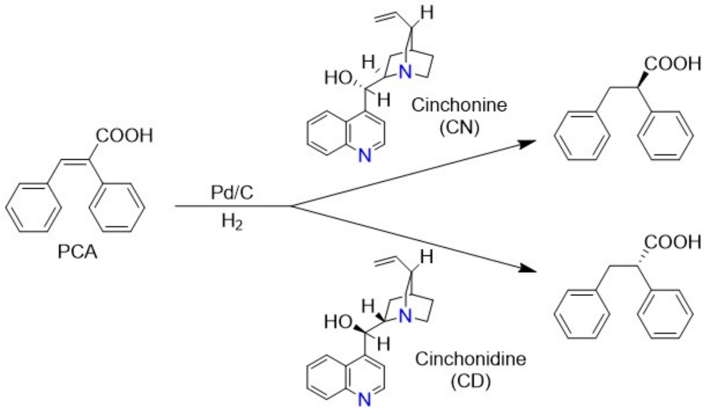

Fig. 13. Cinchonidine (CD) and cinchonine (CN) as chiral modifiers for Pd/C in enantioselective hydrogenation.

Baiker and co-workers used commercial Pt/Al_2O_3 in presence of different modifiers such as NMe_3, NEt_3, Quinuclidine, Quinoline, (*R*,*R*)-PNEA, CD, and *O*-Methyl-CD as additives in the hydrogenation of different substrates [96]. The addition of trace amounts of the chiral modifiers enhanced the chemoselectivity up to 100% in the hydrogenation of activated carbonyl groups with up to 93% *ee*. This study showed a higher adsorption for the chiral ligands than for simple amines and the high chemo- and enantioselectivities were attributed to the formation of an ion pair involving the protonated amine function of the chiral modifier and the enolate form of the substrate.

3. Phosphorus donor ligand-capped heterogeneous catalysts

Another common type of capping agents for heterogeneous catalysts are P-donor ligands. Similarly to N-donor ligands, depending on the focus of the study and the catalytic application, several synthetic strategies were reported to modify the MNP surface with these ligands.

3.1 Colloidal synthesis of P-capped MNPs followed by deposition over a solid support

In order to form well defined MNPs with small size and narrow distribution, one of the most efficient synthetic methods consist in the colloidal formation of the MNPs followed by their deposition onto a solid support. The drawback of this strategy is, in some cases, the weak interactions between the MNPs and the support that can result in the release of the MNPs under catalytic conditions.

For instance, Philippot and co-workers synthesized a series of ligand-stabilized Pd NPs and their subsequent deposition over mesoporous carbon (**Fig. 14**) [97]. The Pd NPs were prepared via the organometallic approach [98] and stabilized with triphenylphosphine or trioctylphosphine [99, 100]. Direct impregnation of the colloids onto the solid support provided the final catalysts which were tested in aerobic oxidation of benzyl alcohol to benzaldehyde, providing excellent conversions and high selectivity to the aldehyde.

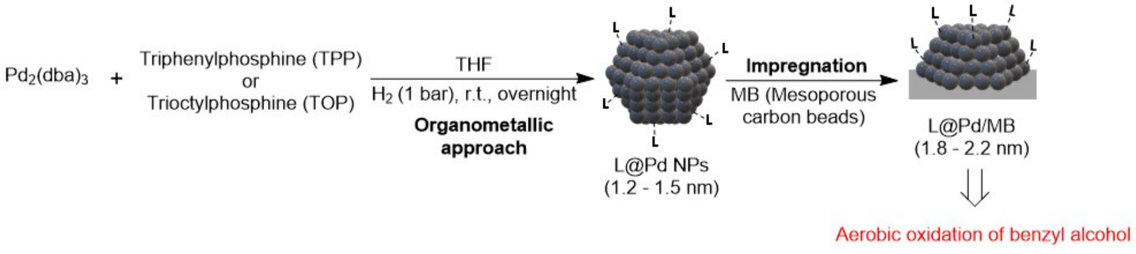

Philippot and co-workers, 2012

Fig. 14. Phosphine-stabilized Ru NPs supported on carbon beads for their application in the aerobic oxidation of benzyl alcohols.

Later, the same group reported a series of carbon-supported Pd NPs for the dual selective aqueous oxidation of benzyl alcohol and the hydrogenation of furfural in water under microwave irradiation [101]. Two synthetic routes for the catalysts were compared: the impregnation of the carbon support with the previously synthesized Pd nanoparticles stabilized with trioctylphosphine and triphenylphosphine as ligands and the impregnation of the support with the palladium metal precursor (in absence of phosphine ligand) followed by hydrogenation. The nanoparticles stabilized by trioctylphosphine followed by their anchoring onto carbon support provided the highest activity. When trioctylphosphine was ligand, the steric hindrance induced by the aliphatic chains limited the interaction between the Pd NPs and the carbon surface oxygen groups, thus preventing their agglomeration that was observed when triphenylphosphine was used. The presence of oxygen groups on the surface of the carbon support improved the Pd NPs immobilization and the water affinity, and consequently enhanced the catalytic performances of the system.

In 2016, Lee and co-workers reported the preparation of Ni NPs by a colloidal method using oleylamine (OAm) and trioctylphosphine (TOP) as stabilizers, and their subsequent deposition over a carbon support. These systems were used as catalysts for the selective hydrogenation of unsaturated furanic aldehydes to their corresponding alcohols [102]. In a previous study, it was reported that OAm was the reductant that controlled the nucleation rate while TOP provides a tunable surface stabilization through its coordination to the Ni surface [103]. The capped nanoparticles provided high selectivities (> 90%) in the hydrogenation of unsaturated furanic aldehydes. In comparison, the uncapped calcined Ni/SiO_2 catalysts presented selectivity to the over-hydrogenation product tetrahydrofurfuryl alcohol. DRIFT results confirmed that the approach of the furanic ring to the Ni surface was limited at the capped nanoparticles due to the steric hindrance induced by the organic surface layer.

In 2012, Serp, Gómez and co-workers synthesized bimetallic platinum–ruthenium nanoparticles stabilized by pyridine- and monophosphine-based ligands and supported over functionalized multiwalled carbon nanotubes in supercritical CO_2 or in THF (**Fig. 15**) [104]. The bimetallic nanoparticles were confined into functionalized multiwalled carbon nanotubes (MWCNT), which led to a higher degree of agglomeration for the PtRu nanoparticles stabilized by phosphine ligands than for those stabilized by the pyridine ligands. These catalysts were applied to cinnamaldehyde hydrogenation and confined PtRu nanoparticles provided higher activity and selectivity than the unsupported nanoparticles.

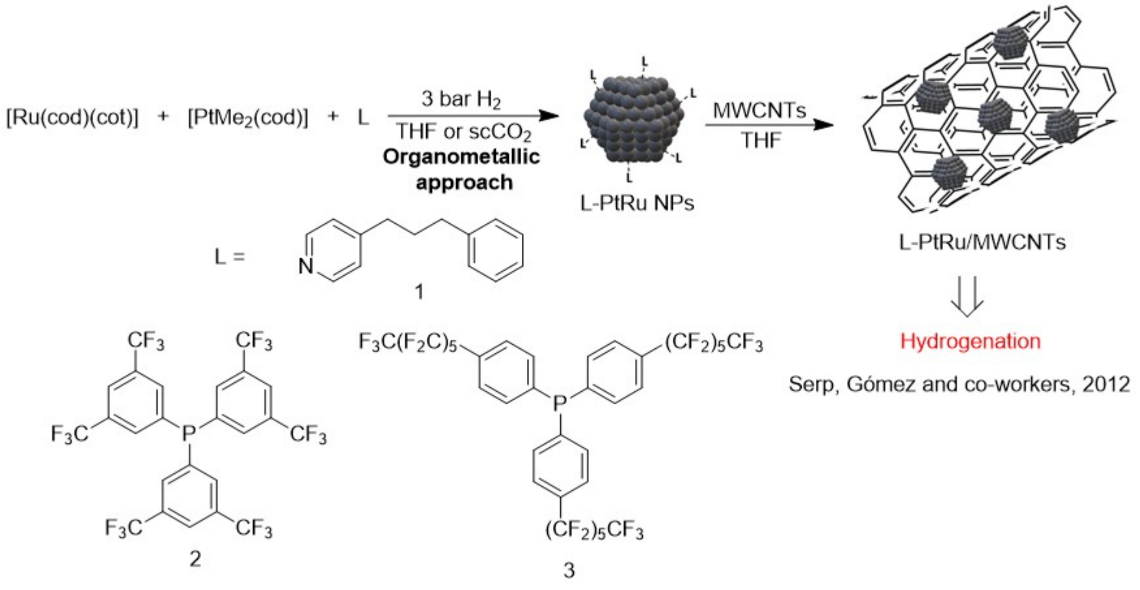

Serp, Gómez and co-workers, 2012

Fig. 15. Preparation of ligand-capped bimetallic platinum–ruthenium hydrogenation catalysts supported over functionalized multiwalled carbon nanotubes.

Ruiz and co-workers synthesized colloidal Rh NPs bearing a chiral ligand ((-)-DIOP) by chemical reduction of the Rh precursor with $NaBH_4$ (**Fig. 16 (a)**) prior to their deposition over SiO_2 [105]. The range of NP sizes were 3.9-5.8 nm depending on the metallic loading and the ligand concentration. When the catalyst prepared in the absence of ligand was used, the diameter of the corresponding MNPs was *ca*. 14 nm, which highlights the stabilization role of the ligand during the synthesis. These MNPs were tested in the asymmetric hydrogenation of acetophenone, 1-phenyl-1,2-propanedione, 3,4-hexanedione, 2,3-butanedione and ethyl pyruvate with *ee's* up to 53%.

The same authors reported a series of Rh NPs stabilized with (*S,S*)-1,2-ethanediylbis[(2-ethoxyphenyl)phenylphosphine] ((*S,S*)-DIPAMP) (**Fig. 16 (b)**) subsequently deposited over SiO_2 [106]. Catalysts formed using various Rh/L ratios were tested in the asymmetric hydrogenation of hexanodione, ethyl pyruvate, ketopantolactone and acetophenone. Good conversion (99%) and enantiomeric excess (*ee* up to 54%) were obtained.

In 2019, they also reported the preparation of Rh NPs (<3 nm) stabilized with a series of P-chiral ligands supported over SiO_2 (**Fig. 16 (c)**) [107].

These systems were tested in 1-phenyl-1,2-propanedione hydrogenation and obtained up to 98% conversion and 67% enantiomeric excess for (*R*)-1-hydroxy-1-phenyl-propan-2-one and 59% for (*R*)-2-hydroxy-1-phenylpropan-1-one.

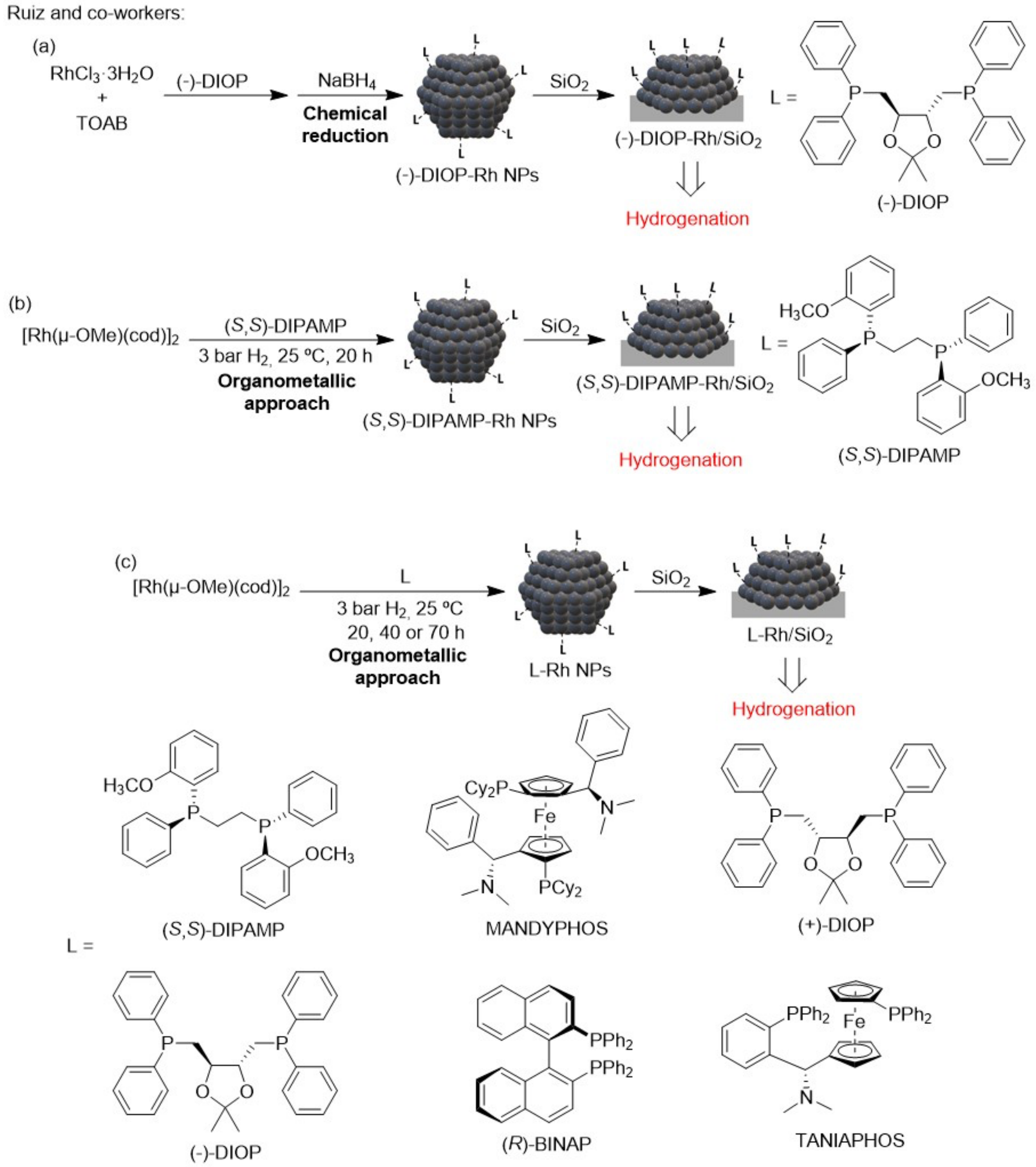

Fig. 16. Asymmetric hydrogenation Rh catalysts stabilized by chiral P-ligands and supported over silica reported by Ruiz and co-workers.

In 2016, Rossi, Philippot and co-workers synthesized a series of Rh NPs stabilized with PVP and mono- and diphosphines (i.e. PPh_3 and dppb) using the organometallic approach [108]. The resulting MNPs presented diameters of 2.2, 1.3 and 1.7 nm, respectively, and were subsequently supported over an amino functionalized silica-coated magnetite.

The colloidal and supported systems were tested in the hydrogenation of cyclohexene. Lower activity was observed for the phosphine-stabilized catalysts due to the blocking of the active sites by the ligands. It is noteworthy that the presence of the phosphine ligands was confirmed even after several recycling cycles of the supported nanocatalysts.

Li and co-workers reported the synthesis of colloidal Rh NPs stabilized by (*R*)-BINAP by chemical reduction with $NaBH_4$ (**Fig. 17**) [109]. The size of these MNPs were between 1.5 and 2.0 nm. The stabilized MNPs were later immobilized by impregnation over silica. The coordination of the ligand was demonstrated by ^{31}P MAS NMR and IR. These systems were tested in the asymmetric hydroformylation of olefins with total regioselectivity and *ee* up to 59%. The supported MNPs exhibited higher activity than the colloidal systems. The system was also successfully recycled and reused upon addition of (*R*)-BINAP ligand after a few runs.

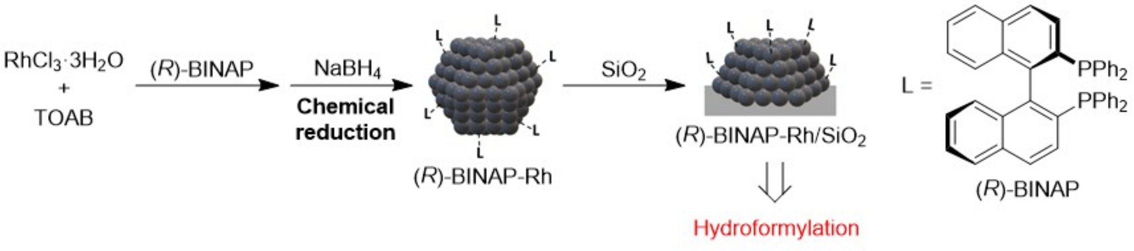

Li and co-workers, 2008

Fig. 17. Preparation of heterogeneous asymmetric hydroformylation catalysts reported by Li and co-workers.

3.2 Colloidal synthesis of P-capped MNPs in the presence of a solid support

Chen and co-workers reported the preparation of Ir NPs by reduction of a metal salt in the presence of PPh_3 and SiO_2 modified with a chiral amine derived from natural cinchona alkaloids (**Fig. 18**) [110]. This catalyst was employed in the hydrogenation of aromatic ketones and provided high activity and high enantioselectivity. The authors later expanded their study with the synthesis of Ir NPs stabilized with a series of phosphines and supported over SiO_2 modified with cinchonine, cinchonidine, quinone and derivates (9-amino(9-deoxy)epicinchonine, 9-amino(9-deoxy)epicinchonidine (1), and 9-amino(9-deoxy)epiquinine) (2) [111]. When cinchonine, cinchonidine, and quinine were used, low catalytic activity and high chemoselectivity to saturated ketone was observed. The best results were obtained when PPh_3 was the ligand used for the stabilization of the catalyst but rather low enantioselectivity was obtained in all cases (up to 46%).

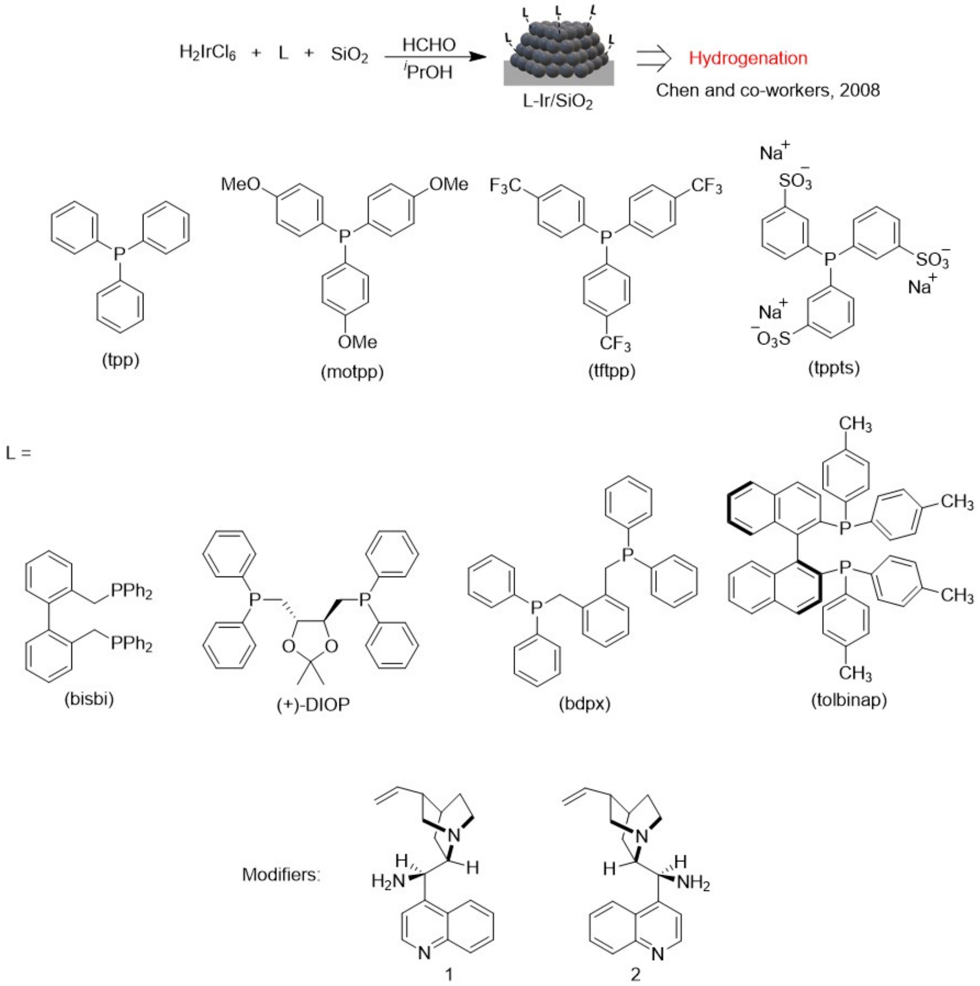

Fig. 18. Preparation of Ir NPs by reduction of a metal salt in the presence of phosphines and SiO_2 modified with a chiral amine.

In 2017, Godard, Taoufik and co-workers prepared by surface organometallic chemistry (SOMC) methodology a series of Rh and Pt NPs ligated by phosphine ligands and supported on phosphine functionalized silica [112]. The presence of the P-donor ligand both in solution and at the support surface revealed important. These systems were employed in the hydrogenation of *p*-xylene, 3-hexyne, 4-phenyl-2-butanone, benzaldehyde and furfural, and demonstrated high activities. Moreover, excellent results were obtained for the selective hydrogenation of furfural to furfuryl alcohol, with high activities in the case of the Pt catalyst. It was concluded that the phosphine stabilized moiety played an important role in the selectivity of this reaction by blocking some surface sites.

Later, the same authors reported the synthesis of monometallic Pd and Cu and bimetallic PdCu NPs stabilized by triphenylphosphine supported over carbon nanotubes (CNTs) and phosphorus functionalized silica (P-SiO_2) [113]. When the support employed was the P-SiO_2, MNP sizes were between 1 and 2.4 nm. However, when CNTs were used, the nanoparticle size was larger, in the range of 2.4-2.6 nm. These catalysts were tested in the semi-hydrogenation of alkynes. PdCu/CNTs was the most active system when the substrates were alkyl substituted alkynes and also showed good recyclability during several cycles.

Godard and coworkers also used this approach to synthesize a Pd based catalyst supported on filter paper [114]. In this work, a Pd precursor was decomposed under H_2 atmosphere in the presence of PCy_3 and CNTs. The resulting material was then used to make an ink via dispersion in water in the presence of a surfactant. Painting of the ink on the filter paper support followed by drying provided a low cost and easy handling catalyst that was applied in the semi-hydrogenation of alkynes and alkynols. Recycling of this catalyst could be performed at least 5 times without loss of activity or selectivity. In 2023, the same group reported a series of Pd NPs stabilized with ligands of different nature (mono- and bidentate phosphines organic and water-soluble and NHCs) (**Fig. 19**) via the organometallic approach in the presence of different supports (metal oxides and carbon-based) [115]. The Pd NPs supported over TiO_2 presented sizes between 1.92 (for PTA) and 2.83 nm (for NHC). When the synthesis of Pd/TiO_2 was performed in the absence of ligand, the particle size was 5.36 nm, demonstrating the beneficial effect of the ligands on the MNP stabilization. All these catalysts were tested in the hydrogenation of CO_2 in basic media to produce formate. The system containing PPh_3 provided the highest catalytic activity (TON = 1032).

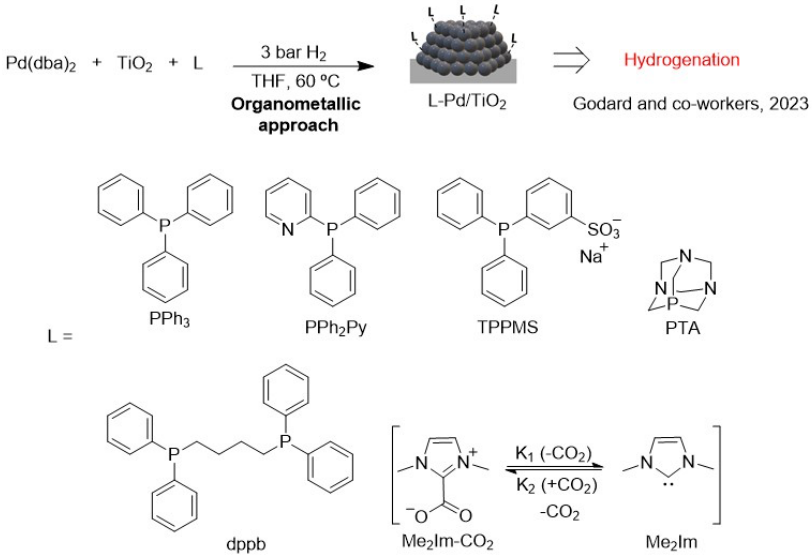

Fig. 19. Preparation of phosphine stabilized heterogeneous Pd catalysts for CO_2 hydrogenation into formate.

In 2008, Xiong and co-workers reported the synthesis of the Ru-phosphine/γ-Al_2O_3 catalyst (*ca*. 5 nm) by reduction of $RhCl_3$ in the presence of the support and the phosphine ligand. For application in catalysis, modification of this material by addition of (1*S*,2*S*)-DPEN was performed. This catalyst was used in the asymmetric hydrogenation of acetophenone and derivatives [116]. The effect of various phosphine stabilizers was examined in catalysis. When the Ru/γ-Al_2O_3 catalyst was stabilized by phosphine ligands, the catalytic activity and enantioselectivity increased. The best results were obtained when PPh_3 was used. Under optimum conditions, total conversion of acetophenone was reached with enantioselectivity up to 78% *ee*. The catalyst could be reused several times and although *ee* was maintained for several cycles, the catalytic activity decreased due to the loss of Ru-PPh_3/γ-Al_2O_3 catalyst during the separation process and the partial oxidation of the PPh_3 stabilizer.

3.3 Functionalization of previously synthesized heterogeneous catalysts using P-donor ligands

In 2000, Anderson and co-workers reported the use of $Rh/SiO_2 \cdot Al_2O_3$ in the presence of the chiral diphosphines [i.e. (-)-Chiraphos and (-)-DIOP] in the hydroformylation of styrene [117]. The catalytic activity was significantly decreased after functionalization with the diphosphines although high chemo- and regioselectivity towards the chiral aldehyde were obtained. Optical yields were moderate (up to 9% *ee*) and dropped to zero when the catalysts were reused. The interactions of these diphosphines with the supported rhodium catalysts were studied after exposing the catalyst to a solution of the P-additive in toluene. Mechanistic investigations revealed the formation of a rhodium gem-dicarbonyl complex, Rh(I)(CO)(P–P) attached to the solid. The modifiers were adsorbed on the support and to a lesser extent on the metal surface. Controlling the water content of the solvent and the degree of hydration of the catalyst surface reduced the Rh leaching.

In 2005, Ding and co-workers prepared Leaching of rhodium a novel heterogeneous Rh/SiO_2 catalyst by impregnation of $RhCl_3$ over commercial SiO_2 through the incipient wetness method followed by calcination. The resulting material was then modified with PPh_3 [118]. This catalyst was employed in the hydroformylation of propylene provided higher catalytic performance than the unmodified heterogeneous Rh/SiO_2 catalyst. Spectroscopic techniques confirmed that PPh_3 molecules were chemically adsorbed at the surface of the modified heterogeneous Rh/SiO_2. The same authors later reported a novel catalyst based on Rh NPs supported over SiO_2 [119]modified with triphenylphosphite ($P(OPh)_3$). This system was employed in the hydroformylation of internal olefins to linear aldehydes and reached high activity and regioselectivity.

In 2009, Yamashita and co-workers synthesized bimetallic FePd NPs by thermal decomposition of iron carbonyl ($Fe(CO)_5$), followed by reduction of palladium acetylacetonate ($Pd(acac)_2$) and using oleic acid and oleylamine as stabilizers [120]. These MNPs contained a Fe_xO_Y-rich core and a Pd-rich shell which was functionalized by ligand exchange with the chiral ligands, (*S*)-BINAP and (*R*)-BINAP. These MNPs exhibited sizes of *ca*. 5.6 nm. These materials were the first example of asymmetric catalytic application using chiral magnetic FePd NPs. They were used in asymmetric Suzuki-Miyaura coupling reaction giving >99% yield in both cases and *ee* values of 48% when (*S*)-BINAP was used and 46% in the case of (*R*)-BINAP.

Felpin and Landais reported the first Pd/C-mediated allylic substitution in water using PPh_3 as additive under catalytic conditions [121]. It was concluded that the phosphine probably acts as a stabilizing agent for Pd, generating *in situ* a more reactive Pd(0)-PPh_3 complex. Finally, an asymmetric version of this new catalytic system was performed using chiral diphosphine ligands. (*R*)-BINAP afforded diethyl 2-[(*E*)-1,3-diphenyl-2-propenyl]malonate in 80% *ee*, albeit in low yield.

In this field, Baiker and co-workers reported the use of commercial Pd/Al_2O_3 (*ca*. 3 nm) modified by chiral ligands (**Fig. 20 (a)**) for their application in asymmetric allylic substitution of (*E*)-1,3-diphenylallyl acetate with dimethyl malonate [122]. The enantioselectivity of the Pd/Al_2O_3-BINAP system [58–60% *ee* to (*S*)-2] was independent of the reaction temperature (60 and 120 °C), and very low amounts of BINAP were required. Surprisingly, the addition of BINAP induced a significant rate acceleration (by a factor of almost 7 at 60 °C) and improved the chemoselectivity of Pd/Al_2O_3. Among the diphosphine ligands tested, (*R*)-Solphos provided the highest enantioselectivity (67% *ee*).

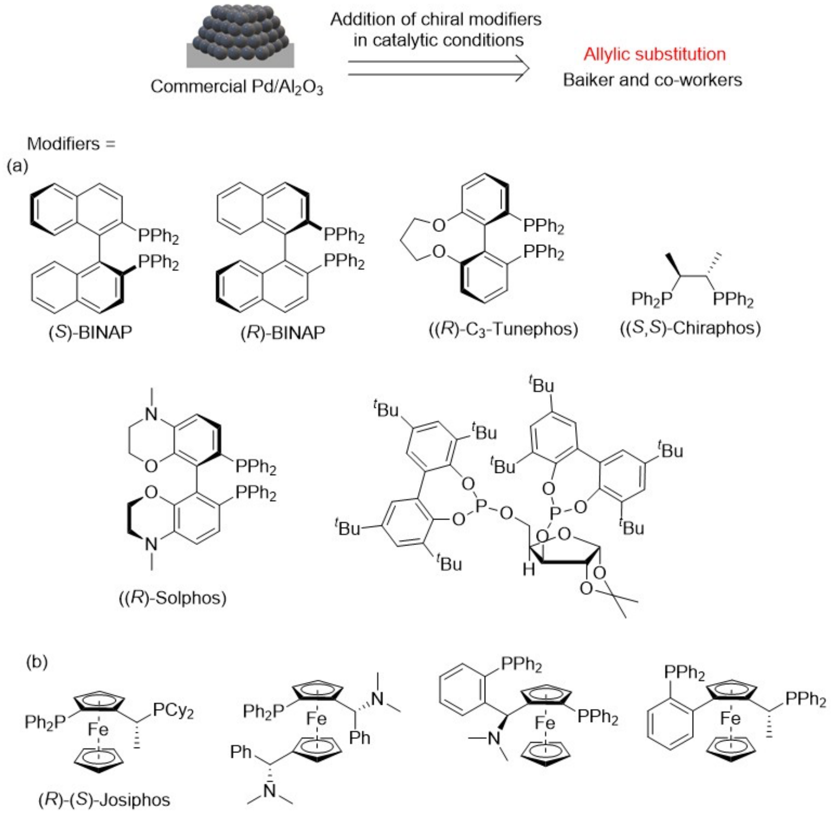

Fig. 20. Modification of commercial Pd/Al_2O_3 for application in asymmetric allylic substitution of (*E*)-1,3-diphenylallyl acetate with dimethyl malonate.

In 2008, the same group reported the use of commercial Pd/Al_2O_3 in the presence of optically active ferrocenyl phosphines (**Fig. 20 (b)**) as chiral modifiers for the enantioselective allylic substitution of (*E*)-1,3-diphenylallyl acetate with dimethyl malonate [123]. These catalytic systems exhibiting good activity along with good enantioselectivity (up to 88% *ee*). Addition of the modifiers to Pd led to significant rate acceleration and in some cases, kinetic resolution of the racemic allylic acetate substrate.

More recently, the same group reported the functionalization of commercial Pd/Al_2O_3 by (*R*)-BINAP for the enantioselective allylic alkylation of (*E*)-1,3-diphenylallyl acetate with enantio-induction in the range 20-30% *ee* (**Fig. 20**) [124].

Using a different approach, Park and Chung prepared colloidal CoRh heterobimetallic nanoparticles (*ca*. 2 nm) by thermal decomposition of cobalt-rhodium carbonyl clusters [i.e. $Co_2Rh_2(CO)_{12}$ and $Co_3Rh(CO)_{12}$] in the presence of oleic acid and trioctylphosphine oxide, prior to their immobilization on charcoal [125]. These catalysts were applied in the Pauson–Khand-type reaction under 1 atm of CO. The catalytic activity depended on the Co:Rh ratio of the bimetallic nanoparticles and the highest activity for intra- and intermolecular Pauson–Khand-type reactions was observed when the ratio was 1. When the catalyst was used in the presence of an aldehyde instead of carbon monoxide, high efficiency was reported. In addition, when the reaction was carried out in the presence of chiral diphosphines, up to 87% *ee* was achieved. The catalytic system could be reused at least five times in the presence of chiral diphosphines (added in catalytic conditions as modifiers) without loss of catalytic activity and enantioselectivity.

In 2007, Zhao and co-workers reported the asymmetric hydrogenation of acetophenone catalyzed by Ru/γ-Al_2O_3 in the presence of PPh_3 and the chiral amine (*R*,*R*)-DPEN, obtaining up to 60% *ee* [126]. The results demonstrated that the phosphine ligand and amine were crucial for this reaction. The catalyst could be reused four times without loss of activity nor enantioselectivity although the addition of the modifier and the ligand together with the substrate was required for the recycling.

Recently, Cui and co-workers employed the combination of the non-noble metal heterogeneous catalyst Ni/Al_2O_3 (*ca.* 5 nm) with the Xantphos ligand as catalytic system in the regioselective hydrosilylation of a wide range of aromatic and aliphatic terminal alkynes with $PhSiH_3$, affording the corresponding (*E*)-vinylsilanes in good to excellent yields with high regioselectivity [127]. Several ligands were employed but the best results were obtained with Xantphos, which was attributed to the efficient modulation of the steric and electronic environment of the supported Ni/Al_2O_3 catalyst by this ligand.

Anderson and co-workers previously reported the preparation of Pd/TiO_2 catalyst by impregnation and subsequently modified via the adsorption of triphenylphosphine for acetylene semi-hydrogenation (**Fig. 21**) [128, 129]. Spectroscopic and theoretical calculations provided evidence for charge transfer from PPh_3 to the metal centers [130, 131] and it has been postulated that the impact of this ligand on a metal surface is to polarize the metal–hydrogen bond and subsequently enhance selectivity in the semi-reduction of alkynes [132].

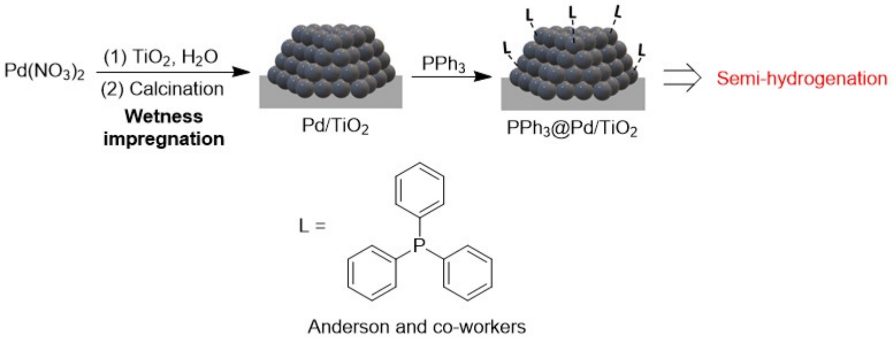

Fig. 21. Preparation and modification of a Pd/TiO_2 catalyst for application in the semi-hydrogenation of acetylene.

Very recently, Ballesteros-Soberanas and Leyva-Pérez reported the use of Pd/C catalyst modified by electron-poor phosphines in the semi-hydrogenation of alkynes [133]. The presence of the ligands increased the catalyst activity by *ca.* 7 folds while the selectivities were comparable to that of the industrial benchmark Lindlar catalyst. In terms of recyclability, when PPh_3 was employed as modifier, the catalyst could be reused up to four cycles without loss of activity or selectivity.

Li and co-workers prepared Rh NPs supported over silica modified with chiral phosphorus ligands (**Fig. 22**) by impregnation methods [134]. Different particle sizes were obtained depending on the metal loading (2.0, 3.0-4.0 and 5.0-6.0 nm for loadings of 1.0, 3.0 and 5.0 wt%, respectively). The coordination of the chiral phosphine to the Rh was demonstrated by ^{31}P MAS NMR and IR spectra of adsorbed CO. These materials were tested as catalysts in hydroformylation reactions. 100% selectivity of branched aldehyde and up to 72% *ee* were obtained in the hydroformylation of vinyl acetate using the (*R*)-BINAP–Rh/SiO_2 catalyst. It is noteworthy that the modification of Rh/SiO_2 with (*S*,*S*)-DIOP resulted in an increased activity for the hydroformylation of vinyl acetate with a TOF of 128 h^{-1}.

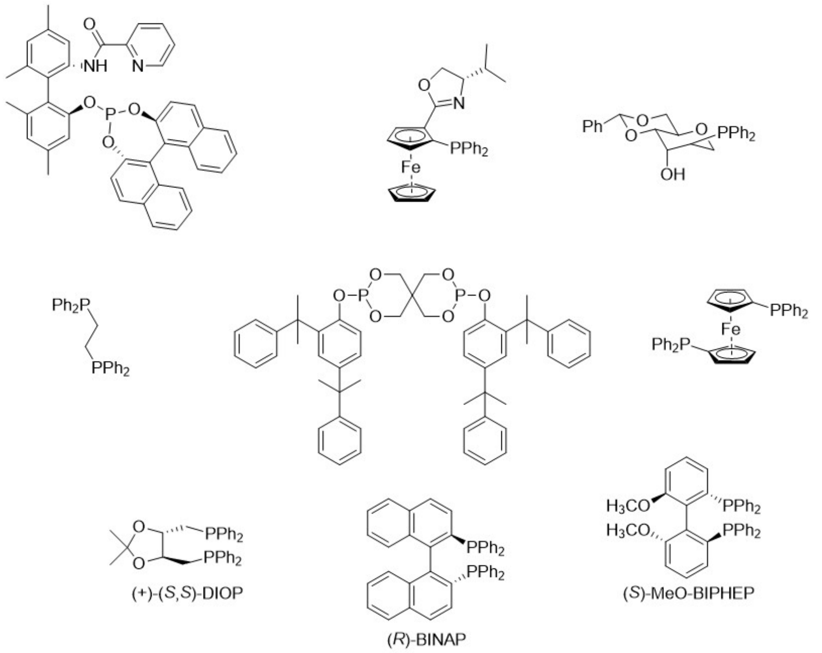

Fig. 22. Chiral phosphorus ligands used by Li and co-workers for the modification of Rh NPs supported over silica.

In 2014, Niemczyk, Polanski and co-workers reported the performance of a bimetallic copper-supported nanopalladium catalyst Pd/PdO/Cu in the Sonogashira coupling reaction using PPh_3 as additive [135]. The presence of the phosphine additive improved the reactivity of the catalyst.

Mika and co-workers reported the use of 5% Ru/C, 10% Pd/C and RANEY Ni CatCart® in the presence of butyl-bis(*m*-sulfonatophenyl)phosphine for the continuous synthesis of γ-valerolactone (GVL) using a continuous-flow reactor [136]. The conversions exceeded 82.9% with 5% Ru/C catalyst, which was further increased to 98.5% by the addition of ligand.

Chatterjee and Jensen reported the use of the heterogeneous commercial Pd/C (*ca*. 20 nm) catalyst in the presence of phosphine ligands for α-olefin formation in deoxygenation of fatty acids [137]. Several phosphines were employed, but best results were obtained using DPEphos as modifiers. The catalyst was recycled at least twice without loss of activity or selectivity. However, after the third cycle, a decrease in activity was observed. This could be attributed to an increase of NP size (*ca*. 70 nm after the 3rd cycle) due to sintering.

In 2021, Hou and co-workers synthesized Pd NPs over mesocellular silica foams by reduction with $NaBH_4$ and subsequent modification with a chiral phosphine [138]. Sizes (from 3.9 to 6.3 nm) could be regulated by increasing $NaBH_4$ reduction times and enlarging support pores. Resulting catalysts were tested in the catalytic intramolecular carboiodination. This was the first report on the asymmetric synthesis of iodomethyl dihydrobenzofuran over supported MNPs. The presence of capping agents positively affected the catalysis outcome by modulation of the size and electronic properties of catalyst surface.

3.4 Functionalization of the support/solvent using P-donor ligands

In 2018, Guo et al. reported the preparation of Pd NPs over a support modified (FDU-12) with PPh_3 by impregnation-reduction method [139]. PPh_3 was cross-linked in the nanopores of a mesoporous silica. Very small Pd NPs were obtained (1.1 nm). Interaction between the phosphine and Pd NPs was demonstrated by XPS, *in situ* FTIR adsorption of CO and D/H exchange reactions. The catalytic performance of this system in hydrogenation reactions was compared with an analogous unmodified material. Interestingly, the activity of Pd NPs was enhanced by the presence of PPh_3 in the hydrogenation of electrophilic nitro compounds.

In 2010, Wang and co-workers synthesized very small Rh NPs (1.8 nm) stabilized by PEG-substituted triphenyl-phopshine [140]. The enhanced stabilization of these MNPs were due to the presence of the PPh_3 groups, and it was evidenced by comparison with MNPs stabilized by PEG. This system was tested in the biphasic hydrogenation of benzene with high activity (TOF= 3333 h^{-1}) and stability. In contrast, the catalyst only stabilized by PEG showed intense aggregation and resulted in very low catalytic activity.

In 2017, Yang and co-workers synthesized a series of Pt NPs over silica modified with triphenylphosphine through an impregnation-reduction method [141]. Very small MNPs were obtained (less than 1 nm) and *in situ* CO adsorption FTIR spectroscopy demonstrated the existence of strong interactions between PPh_3 and Pt NPs. The catalyst in which silica was modified with PPh_3 showed the highest chemoselectivity in the hydrogenation of various substrates compared with other catalysts in which silica was not modified, demonstrating the benefit in terms of stabilization and catalytic performance.

More recently, Yu, Yang and co-workers reported the synthesis of Ru NPs incorporated into silica nanoreactors modified with phosphines and amines [142]. The MNPs were synthesized by chemical reduction with $NaBH_4$ and the particle sizes were *ca*. 2.5 nm.

These systems were tested in the hydrogenation of benzoic acid. In the absence of phosphine, the adsorption of benzoic acid was disfavored and DFT calculations showed that phosphine ligands could modulate the adsorption energy of the benzoic acid over the MNPs tuning their surface.

In 2020, Lei and co-workers reported the synthesis of Pd NPs stabilized with phosphine-functionalized porous inorganic polymer through a two-step approach of anion exchange followed by chemical reduction with $NaBH_4$ [143]. These MNPs were tested in the hydrogenation of nitroarenes with high yield (99.7%) and could be at least 5 times recycled with no significant loss of activity.

In 2021, Philippot and Poli synthesized Rh NPs inside triphenylphosphine-functionalized core-crosslinked micelle latexes [144]. The synthesis was performed by reduction of the Rh precursor with H_2. Rh NPs stabilized with PPh_3 and PEOMA were also synthesized. These systems were tested in several hydrogenation reactions under biphasic conditions. Using this system, the efficient hydrogenation of the vinyl group of styrene was observed. For acetophenone, reduction of both benzene ring and carbonyl reduction was detected. The use of neat 1-octene was also successful, although an increase in activity was obtained when the substrate was diluted in 1-nonanol. For 1-octene hydrogenation, the molecular Rh catalyst was more active than the Rh NPs while when styrene was the substrate, the opposite trend was observed.

In 2022, Doherty, Knight, Chamberlain and co-workers synthesized Ru NPs through impregnation and reduction of the metal precursor over a phosphine and phosphine oxide decorated styrene-based polymer immobilized ionic liquid [145]. This was the first report of RuNPs stabilized by a phosphine oxide-modified support. Very small MNPs were obtained and the catalysts were employed in the hydrogenation of ketones, aldehydes and other substrates such as levulinic acid and ethyl levulinate, with high yields and selectivities. The catalyst in which phosphine oxide is present could be recovered ten times without relevant loss in activity (from 85% to 84%) or selectivity.

In 2010, Rossi and co-workers synthesized Pd NPs over a phosphine-functionalized support ($Fe_3O_4@SiO_2$–iminophosphine–Pd catalyst) [146]. After impregnation of the Pd complex over the previously synthesized support, refluxing conditions led to the formation of Pd NPs [147]. In Suzuki cross-coupling reactions, the catalysts revealed active without the addition of other sources of phosphine ligands. This catalytic system could be easily recovered with the use of an external magnetic field. However, deactivation of the catalyst by etching and MNP aggregation was observed. The addition of the base to the arylboronic acid solution before the introduction of the catalyst solved this issue.

Lu, Chen and co-workers also reported a system based on supported Ru NPs over phosphorus-rich polymer [148]. This system was tested in the reduction of nitro-compounds providing high yields using $NaBH_4$ as reductant.

4. NHC ligand-capped heterogeneous catalysts

4.1 NHC-capped heterogeneous catalysts formed by colloidal synthesis followed by deposition onto a solid support

In 2018, Ravoo and co-workers reported the first preparation of water-soluble NHC-stabilized Au-Pd alloy NPs by ligand exchange (**Fig. 23**) [149]. First, the synthesis of the AuPd NPs was carried out in presence of oleylamine (OAm) as ligand [150, 151, 152]. In a second step, the replacement of the hydrophobic OAm by NHCs was performed by ligand exchange, which led to an increase in Au content of the bimetallic MNPs, probably due to Au atom migration within the MNPs. Subsequently, the deposition over TiO_2 of the NHC stabilized AuPd NPs was carried out. The size of the obtained MNPs varied from 4.1 to 4.6 nm. These systems were applied in semi-hydrogenation reactions with good conversions and selectivities. They were also successfully tested in the hydrogenation of nitroarenes.

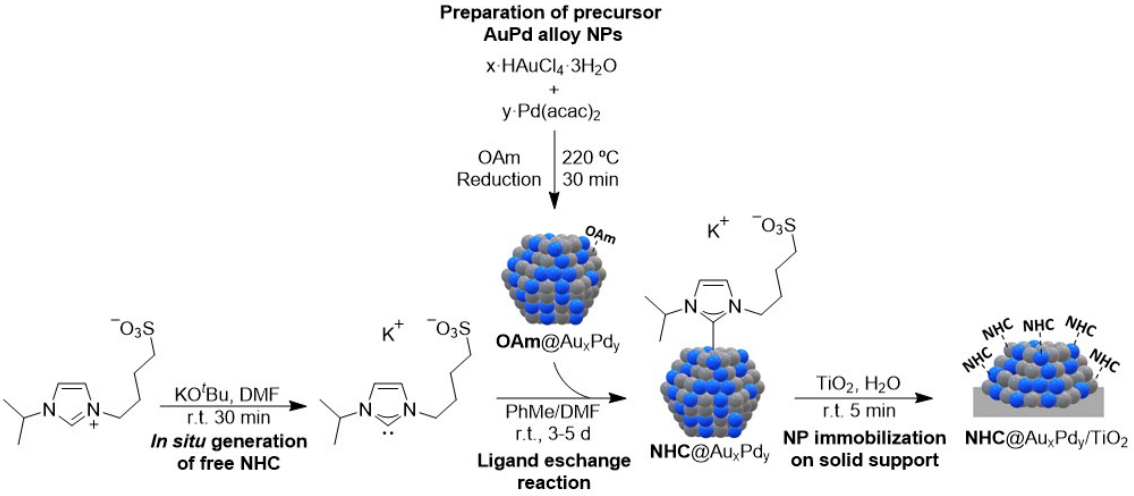

Fig. 23. First preparation of water-soluble NHC-stabilized Au-Pd alloy NPs by ligand exchange.

Ravoo, Evangelisti and co-workers also reported a new strategy including the NHC functionalization of ligand-free Pd NPs previously obtained by metal vapor synthesis and the subsequent dispersion of these NHC-Pd NPs onto a carbon support [153]. This NHC modified system was tested in the hydrogenation of limonene and higher regioselectivity was obtained than when the bare Pd NPs supported over carbon were used.

4.2 NHC-capped heterogeneous catalysts formed by colloidal synthesis in the presence of a solid support

In 2017, Godard and co-workers reported the synthesis of Ni NPs stabilized with NHCs that were obtained by a new methodology involving the decarboxylation of zwitterionic CO_2 adducts and using multiwalled carbon nanotubes (MWCNT) as support (**Fig. 24**) [154]. Immobilization of these Ni NPs in the inner cavity of carbon nanotubes was carried out by hydrogenation of the Ni precursor in the presence of both the NHC precursor and the support. This system was tested in the selective hydrogenation of alkynes into (*Z*)-alkenes, showing excellent activities and selectivities. Moreover, no over-hydrogenation of the Z-alkene products was observed under prolonged reaction times. Later, the same group extended the study to the synthesis of NHC-stabilized CNT-supported monometallic (Cu and Pd) and bimetallic (PdCu and NiCu) MNPs via decarboxylation of imidazolium carboxylate adducts (**Fig. 24**) [155]. In terms of size (2-7 nm), the trend was that the supported MNPs were slightly smaller than the colloidal ones in all cases, except the NiCu NPs. These systems were tested in the semi-hydrogenation of alkynes and alkynols. PdCu/CNTs revealed highly selective in the hydrogenation of terminal and internal alkynes and showed high stability in the semi-hydrogenation of acetylene in acetylene/ethylene-rich feeds.

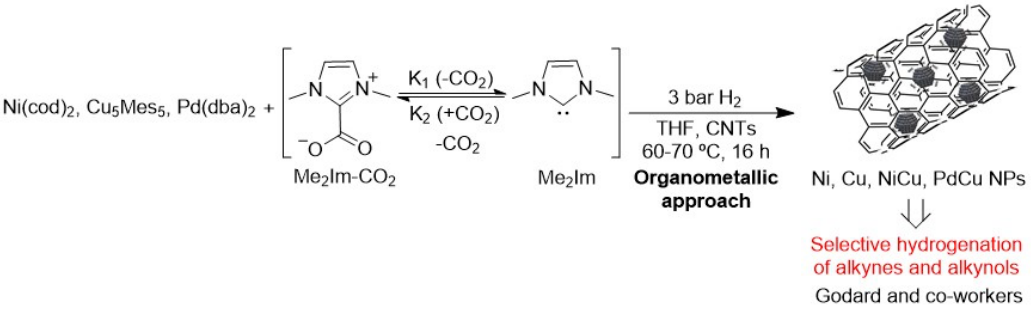

Fig. 24. Preparation of NHC-stabilized mono- and bimetallic MNPs supported on MWCNT by decarboxylation of imidazolium carboxylate.

In 2018, Borja, Mata and co-workers synthesized Pd NPs by decomposition of palladium complexes stabilized by NHC ligands, which were previously anchored onto the surface of reduced graphene oxide (rGO) (**Fig. 25**) [156]. These systems were successfully employed in the semi-hydrogenation of alkynes and could be recycled up to ten times with no relevant loss in activity. Very recently, Guisado-Barrios, Mata and co-workers synthesized a similar catalyst (**Fig. 25**) [157]. This system was tested in the hydrogenation and dehydrogenation of N-heterocycles without additives. In this case, the ligand did not only act as stabilizer of the Pd NPs, but also played a role in the π-interaction with the support, increasing the catalyst stability. Moreover, the support (rGO) also acted as carbocatalyst in the acceptorless dehydrogenation of N-heterocycles. This catalyst demonstrated high stability and could be recycled eight times without loss of activity.

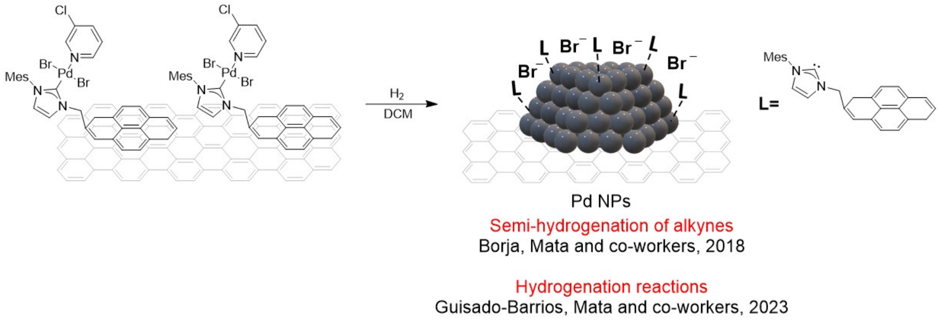

Fig. 25. Synthesis of NHC-capped heterogeneous Pd catalysts by decomposition of anchored palladium NHC complexes at the surface of reduced graphene oxide (rGO).

In 2018, Oberhauser and co-workers prepared Ir NPs stabilized by a bulky NHC [158]. However, when the catalyst was produced in the presence of carbon support (C^K), the NHC stabilizer could not be detected. These systems were tested in the oxidation of glycerol into lactic acid in the presence of NaOH. The colloidal system gave high selectivity to the lactic acid (93%) and good recyclability even under air.

In 2019, Fadakar and co-workers synthesized a new hybrid nanoporous material based on Pd NPs (50–200 nm determined by SEM) stabilized by an NHC ligand and supported on a zeolitic imidazole framework [159]. The procedure for the synthesis of these new materials was based on the impregnation of the NHC-palladium precursor over the support, followed by a reduction using $NaBH_4$. These materials were tested in the Suzuki-Miyaura cross-coupling reaction and provided high activity and stability.

4.3 Functionalization of previously synthesized heterogeneous catalysts using NHC ligands

Recently, Liu, He and co-workers modified previously synthesized supported Au and Pd NPs by addition of polymers containing NHC ligands (mono- and polydentate) [160] and compared their performance in the CO_2 electroreduction with analogous catalysts modified by oleic amine and thiols (**Fig. 26**). The Pd catalysts containing OA and DT were less selective for CO_2 reduction. The highest activity was obtained for the system based on Au NPs, although, in both cases, the presence of the polymeric NHCs resulted in higher activities compared with the unmodified Au/C and Pd/C catalysts. The authors indicated that the polymeric NHCs formed a layer that does not only stabilize the MNPs against sintering, but also promote CO_2 reduction by limiting proton diffusion and binding to MNPs. As a result, the selectivity for CO_2 reduction was relevantly improved due to the hydrophobicity of the polymer ligands and the higher surface electron density of MNPs through σ-donation from NHCs.

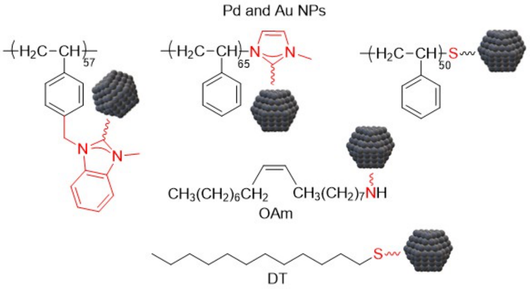

Fig. 26. Au and Pd catalysts modified by addition of polymers containing NHC ligands.

In 2020, Pieters and co-workers reported new air-stable catalysts based on the commercial Ru/C system modified by NHCs [161]. The coordination of the carbenes was confirmed via the use of ^{13}C-labelled NHC ligands and subsequent analysis by solid-state ^{13}C MAS-NMR. TEM analysis demonstrated that the morphology of the Ru NPs was not affected by the NHC modification. These catalysts were employed in C-H deuteration reactions. Depending on the Ru/NHC ratios, the reactivity of these systems could be tuned. The NHC modification increased the catalyst chemoselectivity and regioselectivity in the deuteration of alcohols and allowed the synthesis of pharmaceutically relevant deuterated heterocycles (i.e. azine, purine) that are completely reduced using unmodified commercial catalysts. Moreover, a novel reactivity was revealed for such heterogeneous Ru catalysts, namely the selective C-1 deuteration of aldehydes.

In 2022, Martínez-Prieto and co-workers reported the synthesis of graphene-supported Ru NPs (*ca*. 1.5 NPs) that were tuned by the modification of their metal surface with pyrene-tagged NHCs ligands [162]. XPS analysis showed that NHC ligands were present as protonated carbenes, coordinated to the Ru surface and interacting with the graphene support. Moreover, colloidal Ru NPs were also synthesized to study the coordination of the ligand [163]. These systems were tested in the hydrogenation of various molecules of interest. At high surface coverage, the activity of the catalyst was reduced, but the selectivity was enhanced.

In 2016, Muratsugu, Glorius and co-workers reported for the first time the extensive characterization of an NHC-modified supported heterogeneous catalysts (**Fig. 27 (a)**) [164]. The modification was carried out over the previously synthesized Ru/K-Al_2O_3 catalyst [165]. The modification with NHCs did not induce structural changes in the catalyst, even upon variations of the Ru/NHC ratios. The bond between the carbene ligands and Ru was probed by solid-state ^{13}C MAS-NMR. The resulting catalysts were tested in hydrogenation of acetophenone, *trans*-stilbene and phenylacetylene. In the hydrogenation of *trans*-stilbene, a decrease in the conversion was observed at high NHC to surface Ru ratios, although the extent of this variation was dependent on the nature of the NHC ligand. In contrast, in the hydrogenation of acetophenone, a decrease in activity was already observed at lower NHC to surface Ru ratios. The reduced activity observed upon NHC addition was explained by the blockage of active sites of the catalyst by the NHC.

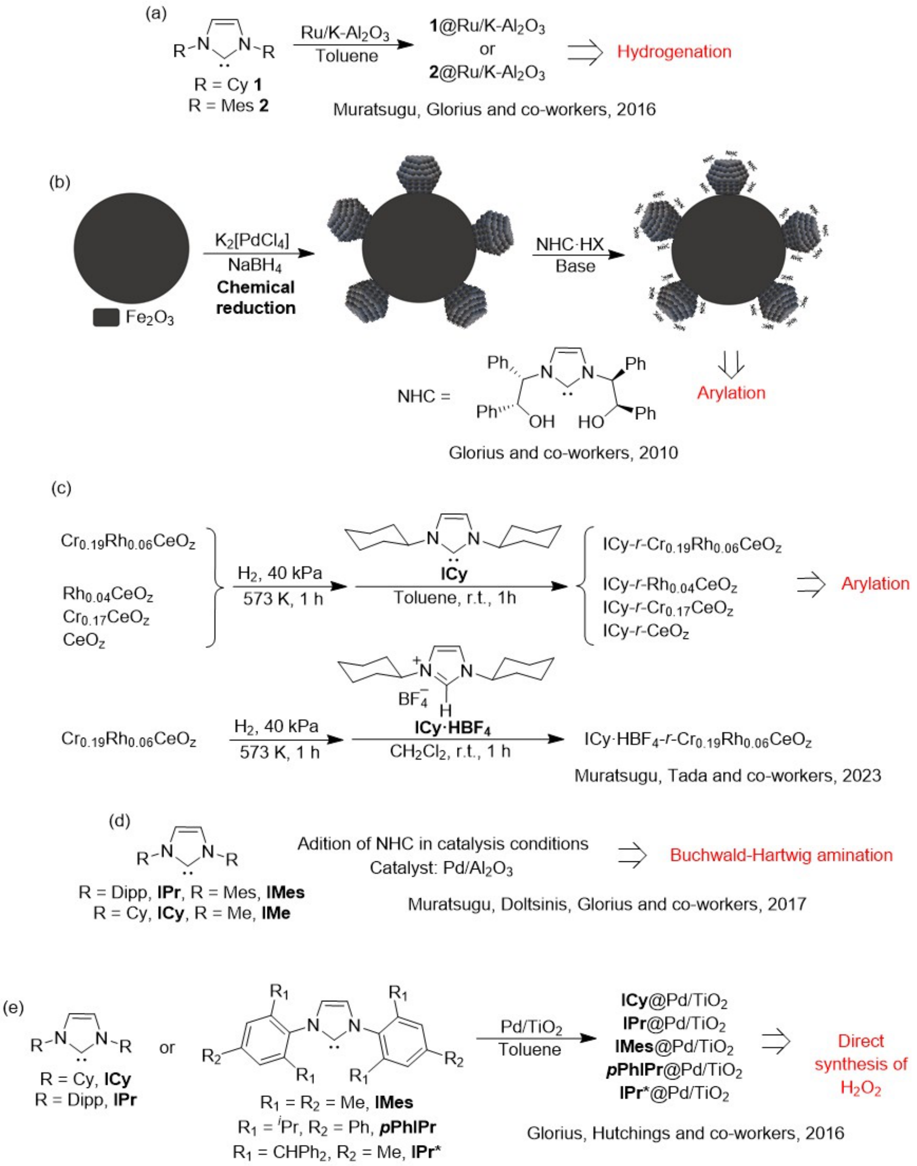

Fig. 27. Synthetic approaches used by Glorius and co-workers for the preparation of NHC-capped catalysts.

In 2010, Glorius and co-workers synthesized Pd NPs by chemical reduction of a palladium salt with $NaBH_4$ over magnetite (Fe_3O_4) [166]. They subsequently carried out the modification of this material using enantiomerically pure NHCs (**Fig. 27 (b)**) [167]. These functionalized-MNPs were tested in asymmetric α-arylation reactions reaching *ee's* up to 85%. Moreover, these catalysts could be separated by magnetic removal from the reaction media and no loss of activity nor selectivity was observed after several cycles.

Very recently, the same group reported the modification of a ceria-based catalyst incorporating Cr and Rh with NHCs (**Fig. 27 (c)**) [168]. The synthesis of the $Cr_{0.19}Rh_{0.06}CeO_z$ was performed by hydrothermal method [169] and followed by the modification with NHCs onto H_2-reduced $Cr_{0.19}Rh_{0.06}CeO_z$. These systems were tested in the 1,4-arylation of cyclohexanone with phenylboronic acid. When the NHC employed was 1,3-dicyclohexylimidazol-2-ylidene (ICy), high activity was obtained. However, in the absence of NHC ligand, the catalyst was inactive. DFT calculations were performed and suggested that the ICy controlled the adsorption sites of the phenyl group on the Rh nanocluster promote the C−C bond formation of the phenyl group and cyclohexanone.

Glorius and co-workers also reported the modification of Pd/Al_2O_3 NPs with NHCs [170]. The NHC was directly added in the catalytic Buchwald−Hartwig amination of aryl halides (**Fig. 27 (d)**). Additionally, further insights into the electronic effect of the coordination with the NHC was obtained by precise characterization of the catalyst surface and *ab initio* calculations.

In 2022, Glorius, Hutchings and co-workers reported a heterogeneous Pd/TiO_2 catalyst modified by NHCs (2.4 nm) (**Fig. 27 (e)**) [171]. The Pd/TiO_2 (2.0 nm) system was first prepared by wet-impregnation method prior to the NHC modification [172]. The systems were tested in the direct synthesis of hydrogen peroxide (H_2O_2) in the absence of promoters. Depending on the NHC substituent, activity could be improved compared with the unmodified catalyst due to the ability of the NHC to electronically modify Pd NPs. Moreover, the modification had a positive effect on the recyclability of the catalysts.

Levratovsky and Gross reported the functionalization of previously synthesized Pt NPs (100 ± 30 nm) supported over SiO_2 with NHCs [173]. Pt NPs were synthesized by the deposition of a Pt film over a Si (110) surface which was coated with a layer of SiO_2. Subsequent modification with NHCs was carried out. The formation of a carbene self-assembled layer onto the surface of the Pt nanoparticles was confirmed and its stability under oxidizing conditions studied by infrared measurements.

In 2018, Wen, Chang and co-workers reported the modification of Pd electrodes with NHCs for the electrochemical reduction of CO_2 [174]. When the tris-N-heterocyclic carbene ligand modified Pd electrode was employed, a 32-fold increase in activity was measured in the electrochemical reduction of CO_2 to C1 products, observing a high Faradaic efficiency compared to the unmodified sample.

4.4 *Functionalization of the support by NHC ligands prior to MNP formation*

In 2009, Jia and co-workers immobilized Pd NPs onto NHC modified mesoporous SBA-15 by a post-grafting route [175]. First, a Pd bromide complex coordinated to the supported NHC ligand was formed, which, upon reduction under H_2 at 200 °C, yielded Pd NPs with a diameter of *ca*. 3.5 nm bearing NHC ligands. Both the initial complex and the resulting MNPs were tested in the aerobic oxidation of benzyl alcohol. The MNP-based catalyst showed much higher activity and could be recycled up to 8 times despite a slight loss in activity.

In 2011, Glorius and co-workers reported the immobilization of an enantiomerically pure imidazolium salt on the surface of magnetite (Fe_3O_4) and the formation of three catalyst of different nature: an organocatalyst, a molecular Pd complex and Pd NPs [176]. The Pd NPs were obtained by chemical reduction in water using hydrazine as reductant. All of them were tested in the allylation of 4-nitrobenzaldehyde, resulting in enantioselectivities between 43 and 74% *ee*´s.

In 2016, Ervithayasuporn and co-workers described a new synthetic methodology for the fabrication of polyhedral oligomeric silsesquioxane-supported NHC/imidazolium salts palladium(II) complexes [177]. Upon addition of phenylboronic acid as reductant, the resulting Pd NPs exhibited a diameter of 3.0 ± 1.5 nm. This material was employed in the Suzuki-Miyaura cross-coupling reactions with high efficiency and could be reused up to ten times without losing activity.

In 2013, Kobayashi and co-workers synthesized a series of Ni NPs over polymer supports which incorporated NHC ligands [178]. The synthesis of the Ni NPs was carried out by the reduction with triethylborohydride ($LiEt_3BH$) and their sizes were between 1 and 4 nm. The presence of the embedded NHCs was checked by NMR analysis and these systems were tested in Corriu-Kumada-Tamao reactions with good results for a wide range of substrates. Moreover, the catalyst could be recycled several times without loss of activity.

5. S-donor ligand-capped heterogeneous catalysts

In view of the ability of S-donor molecules to stabilize group 11 metals and their strong coordination on metal surfaces, S-based ligands were also reported to enhance the catalytic performance of heterogeneous catalysts.

5.1 S-ligand-capped heterogeneous catalysts formed by colloidal synthesis followed by deposition onto a solid support

The first example using this synthetic methodology was reported by Obare and co-workers who described the synthesis of colloidal Pd NPs by thermal decomposition of $Pd_3(OAc)_6$ in the presence of thioethers as stabilizing ligands (sizes: 1.7 - 3.5 nm) [179]. The Pd NPs were subsequently immobilized over commercial SiO_2 and the resulting catalysts evaluated in the hydrogenation of styrene, cyclooctadiene and 6-bromo-1-hexene (**Fig. 28**). The results revealed that the MNP size was a key parameter for catalytic performance as the smallest nanoparticles provided the highest activity. Moreover, these heterogeneous systems were robust since they could be recycled up to 8 times without loss of activity or selectivity.

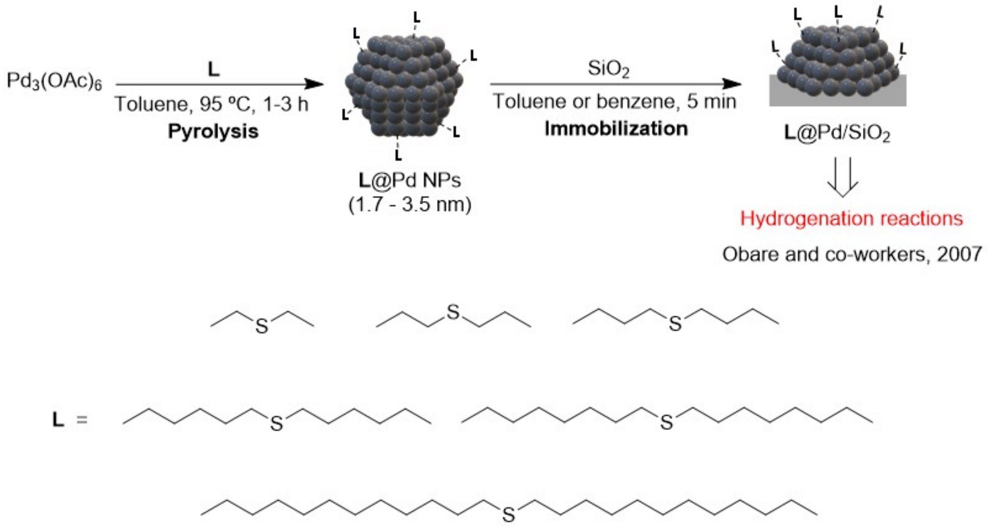

Fig. 28. Colloidal formation of S-donor ligand-capped Pd hydrogenation catalysts followed by deposition over silica.

In 2012, Khlobystov reported the use of Rh and RhPt NPs (≈3 nm) supported over hollow graphitized carbon nanofibers (GNF) and stabilized with sodium S-dodecylthiosulfate (SSDS) in the hydrosilylation of terminal alkynes [180]. Colloidal MNPs were first prepared prior to their deposition over of the support (**Fig. 29**) [181]. Variations in the conditions for the deposition of the MNPs yielded two distinct catalysts containing the active phase either at the surface of the nanofibers or confined within the walls of the support. The regioselectivity was affected by the confinement of the MNPs and depending on the nature of the substituents at the substrates, three main trends were observed while using the confined catalysts: 1) when the reagents did not contain aromatic moieties, no confinement effect was observed; 2) when only the alkyne contained an aromatic substituent, a higher selectivity to dehydrogenative silylation products was observed together with a decrease in the β-(*Z*): β-(*E*) isomers ratio; 3) when both reagents possess aromatic groups, the resulting interactions favored the formation of the thermodynamically less stable β-(*Z*) regioisomer.

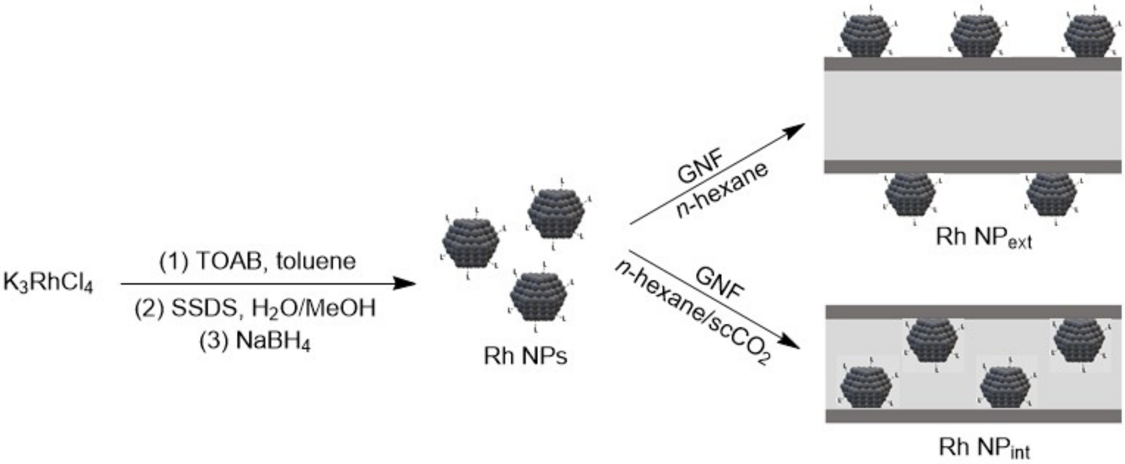

Fig. 29. Preparation of Rh alkyne hydrosilylalation catalysts supported either at the surface or within the cavity of hollow carbon nanofibers.

In 2013, Lopez-Sanchez and co-workers reported the synthesis of colloidal Rh NPs (3 - 5 nm) stabilized by 1-octadecanethiol (ODT), polyvinyl alcohol (PVA), and tetraoctylammonium bromide (TOAB), and their subsequent immobilization for application in hydrogenation reactions [182]. These nanoparticles were immobilized over silica-coated magnetic MNPs modified with 3-aminopropyltriethoxysilane, 3-mercaptopropyltriethoxysilane and thiol [183]. Both colloidal and supported MNPs were tested in the hydrogenation of cyclohexene. Distinct results were obtained according to the stabilizing agents since Rh–ODT NPs were inactive, Rh–PVA NPs exhibited distinct activities in solution (aqueous biphasic catalysis) and as a supported catalyst, while colloidal Rh–TOAB NPs exhibited similar activities with their supported counterpart. Additionally, the stability of the nanoparticles depended on the nature of the ligand modifier and on the functionalization of the support surface before immobilization. The highest turnover frequencies (up to 700,000 h^{-1}) were observed for the colloidal catalyst Rh–TOAB that resulted stable and recyclable.

In 2014, Kunz and co-workers studied the influence of organic ligands on the geometric and electronic surface properties of colloidally prepared Pt nanoparticles (Pt NPs) (1.8 ± 0.3 nm) stabilized with dodecylamine (DDA) and dodecylthiol (DDT) [184]. These MNPs were subsequently supported over TiO_2 and a surface study was carried out by means of diffuse reflectance infrared spectroscopy (DRIFTS) using CO as probe molecule. Marked differences were evidenced according to the stabilizing agent used. The amine capping agent provided an electronic donor influence and a geometric effect, while the thiol was mainly geometric in nature. Moreover, DDA was only weakly adsorbed and could therefore be displaced by strongly binding adsorbates (*e.g.*, CO), while a strong coordination of DDT at the particle surface was observed, forming an uniformly distributed capping layer. The influence of both ligands on the catalyst selectivity in the hydrogenation of crotonaldehyde was also investigated. For amine-functionalized MNPs the catalytic results were similar to those of “unprotected” Pt NPs. In contrast, an enhancement of the selectivity was evidenced for thiol-functionalized particles.

More recently, Chen, Lian and co-workers modified Pt NPs prepared in basic solutions of glycol using a series of stabilizers such as triphenylphosphine (PPh_3), octadecylamine (ODA), poly(vinylpyrrolidone) (PVP), poly(vinyl alcohol) (PVA) and dodecanethiol (DT), prior to their deposition over activated carbon [185]. These materials were tested in the hydrogenation of *para*-chloronitrobenzene (*p*-CNB). Direct or indirect interactions between nanocrystals and stabilizers affected their catalytic performance. The electron-donating ability of the capping agents directly altered the surface electronic state of Pt nanocrystals and consequently affected the adsorption and reactivity of reactants, intermediates and products. Interestingly, using DT as stabilizer, the coordinated Pt atoms were oxidized to generate cationic Pt species at the surface of the nanocrystals, which improved both the hydrogenation rate and selectivity to *para*-chloroaniline.

5.2 Functionalization of previously synthesized heterogeneous catalysts using S-donor ligands

The strong coordination of S-donor ligands was mainly utilized to tune the selectivity of heterogeneous catalysts. However, in some cases, the activity of these catalysts was affected.

For instance, Rusling, Suib, He and co-workers reported the synthesis of Au, Pt and Pd catalysts supported on N-doped carbon by chemical reduction of metallic precursors with $NaBH_4$ [186]. These catalysts were subsequently modified by 3-mercaptopropionic acid (MPA) or dodecanethiol (DT). However, after comparison of their catalytic performance in electrocatalytic oxidation of methanol with the unmodified catalysts, the authors concluded that the presence of the modifiers had a negative effect in terms of activity.

In contrast, McKenna and Anderson reported the modification of a Pd/TiO_2 catalyst with diphenyl sulphide for testing in acetylene hydrogenation (**Fig. 30**) [187]. The Pd/TiO_2 catalyst was prepared by incipient wet impregnation and after calcination of the material, the modification was carried out by addition of an hexane solution of the diphenyl sulphide. The modification of the catalyst resulted in an enhancement of the selectivity to ethylene by inhibition of the over-hydrogenation process. Interestingly, even after thermal treatments which led to decomposition of the adsorbed phenyl sulphide, the remaining sulphur could enhance the selectivity in mixed acetylene/ethylene feed streams.

In a similar study, Anderson and co-workers reported the use of triphenylphosphine and diphenyl sulfide as modifiers of Pd/TiO_2 catalysts in the selective hydrogenation of acetylene from ethylene rich feed-streams at high pressures and in the presence of CO (**Fig. 30**) [188]. Pd/TiO_2 was synthesized by incipient wet impregnation prior to deposition of the modifiers. Initial ethylene selectivities of 85 - 92% were obtained with acetylene conversions up to 100%. Given the differences in the steric and electronic properties of the surface modifiers, the origin of the enhanced selectivity was attributed to the creation of ensembles of Pd atoms able to readily accommodate acetylene but limit the access of ethylene at the metal surface. The use of diphenyl sulfide enhanced ethylene selectivity but also increased the conversion of acetylene. However, the by-product formation was appreciably higher than with the unmodified or triphenyl phosphine modified catalysts.

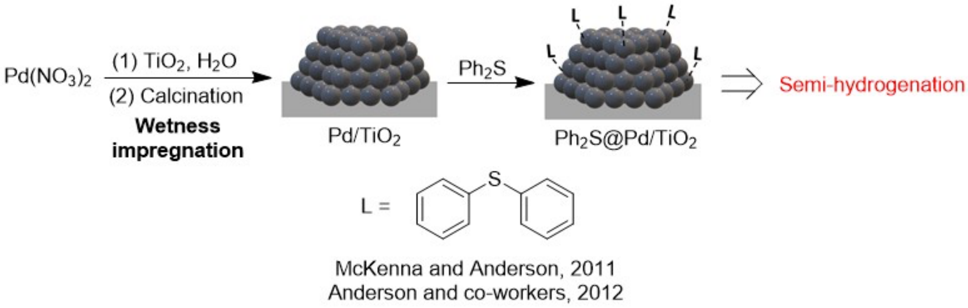

Fig. 30. Preparation of diphenyl sulfide modifieds Pd/TiO_2 catalysts for the semi-hydrogenation of acetylene.

Sajiki and co-workers also reported the modification of commercial Pd/C by diphenyl sulfide and its application in chemoselective hydrogenation reactions [189]. Using this system, olefin, acetylene, nitro, and azide functionalities were efficiently hydrogenated. In contrast, aromatic carbonyl and halide, benzyl ester and N-Cbz functionalities were not. The enhanced chemoselectivity observed were explained by the partial interaction between the active sites of the Pd surface with Ph_2S (i.e. Pd-S bonding). The catalyst could be recovered and reused at least five times without any significant loss of the reactivity.

In 2012, Bokhoven and co-workers reported the modification of Pt/TiO_2 (unmodified: 1 nm and modified: 1.4 nm) with organic thiols for the hydrogenation of 4-nitrostyrene [190]. The Pt/TiO_2 catalyst was synthesized by wet incipient impregnation and functionalized by thioglycerol, 1,6-dithiolhexane, α-lipoic acid and 1-dodecanethiol. The use of a modifier containing a polar group adjacent to the chain of the organic thiol provided higher selectivities and the best results in terms of activity and selectivity were obtained using 1,6-dithiolhexane as modifier.

The group Medlin and co-workers reported the modification of several heterogeneous catalysts with S-donor ligands for various catalytic applications (**Fig. 31**). In 2012, they described the coating of Pd/Al_2O_3 and Pt/Al_2O_3 catalysts with thioglycerol, octadecanethiol, dodecanethiol, hexanethiol, and propanethiol for the hydrogenation of epoxybutene [191]. Depending on the nature of the thiol used, positive or negative effects on activity and selectivity was observed. Coatings with 1-octadecanethiol resulted in marked improvements in selectivity in the liquid phase hydrogenation of epoxybutene. Interactions of the solvent with the self-assembled monolayer (SAM) were also important in controlling selectivity.

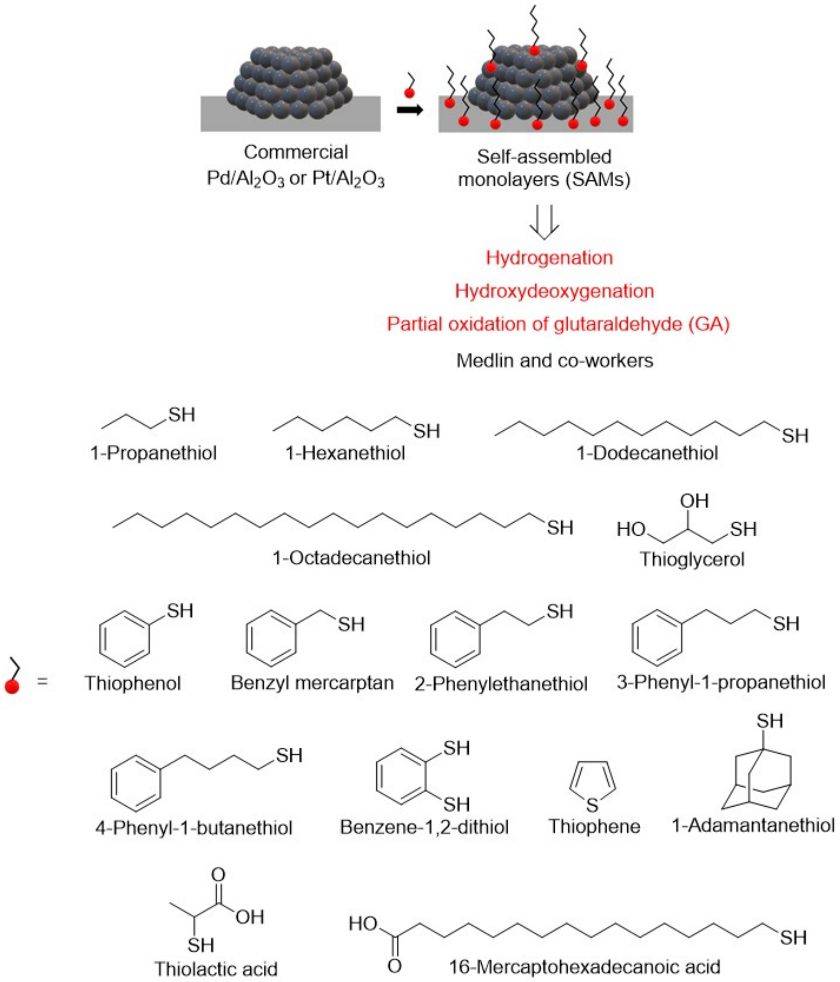

Fig. 31. Modification of heterogeneous catalysts with S-donor ligands reported by Medlin and co-workers.

Later, the same authors used thiolate (1-octadecanethiol and 1-adamantanethiol) self-assembled monolayers (SAMs) as modifiers on commercial Pd/Al_2O_3 (6.7 nm) catalysts (**Fig. 31**) for their use in hydrogenation reactions [192]. In acetylene hydrogenation, the modification by thiols did not provide improvements. In contrast, for reactions where coking is less problematic, the reactivity of the catalysts could be tuned using SAMs and fir instance, ethylene hydrogenation was much faster on adamantanethiol-coated surfaces than on C18-coated surfaces, which was attributed to the impediment of active sites using C18-modified surfaces.

The modification of commercial Pd/Al_2O_3 catalyst with alkanethiol SAMs (i.e. 1-propanethiol, 1-hexanethiol, 1-dodecanethiol, 1-octadecanethiol and thioglycerol) was also applied in the partial hydrogenation of 18-carbon polyunsaturated fatty acids (**Fig. 31**) [193]. While the use of the bare Pd/Al_2O_3 catalyst led to the fast formation of saturated fatty acid, the addition of alkanethiol SAMs increased the reaction selectivity to the monounsaturated product oleic acid up to 80−90%, even at high conversions. This effect was attributed to steric effects between the SAMs and reactants.

Similarly, Pd/Al_2O_3 catalysts coated with 1-octadecanethiol (C18), and benzene-1,2-dithiol (BDT) SAMs were applied in the hydrogenation of furfural [194]. Addition of these surface modifiers systematically increased the hydrogenation selectivity of furfural to furfuryl alcohol and methylfuran.

In 2014, the same authors reported the modification of commercial Pt/Al_2O_3 (Pt particle size: 3.9 ± 1.1 nm for 5wt % Pt/Al_2O_3 and 0.8 ± 0.1 nm for 0.5wt % Pt/Al_2O_3) with thiolate self-assembled monolayers (SAMs) (**Fig. 31**) [195]. The selective hydrogenation of both prenal and cinnamaldehyde substrates to the corresponding unsaturated alcohols was enhanced using thiol-modified catalysts. However, it is noteworthy that the selective hydrogenation of cinnamaldehyde was further controlled through interactions of the substrate phenyl ring with the aromatic ligands of the SAM layer.

Later, they reported the use of 3-phenyl-1-propanethiol, thiophenol and 1-octadecanethiol for covering the surface of commercial Pt/Al_2O_3 (**Fig. 31**) [196]. These systems were tested in the selective hydrogenation of cinnamaldehyde. Once again, the presence of modifiers enhanced the selectivity of the reaction but upon recycling, redeposition of the thiol modifier was necessary to maintain the efficiency of the process.

In 2016, Lien and Medlin reported the use of a mixture of modifiers (1-adamantanethiol (AT) and 1-octadecanethiol (C18)) (**Fig. 31**) on commercial Pd/Al_2O_3 for the benzyl alcohol hydrodeoxygenation [197]. The authors varied the relative amounts of modifiers and looked at the effects on catalyst performance. Compared with the performance of the unmodified catalyst, the use of AT as sole modifier improved both the selectivity to toluene and the activity. As the fractional C18 coverage increased, the selectivity to toluene increased and the selectivity to benzene decreased at the cost of activity. The authors showed that at higher C18 coverage, the availability of terrace sites was reduced due to selective poisoning, inhibiting the decarbonylation to benzene.

In a similar study, the same authors deposited thiol self-assembled monolayers (SAMs) onto Pt/Al_2O_3 catalyst for benzyl alcohol hydroxydeoxygenation (HDO) [198]. These SAMs consisted in the use of 16-mercaptohexadecanoic acid (MHDA) and tetraethylammonium (TEA) (**Fig. 31**). The density of the SAM affected the catalyst activity and the hydrodeoxygenation (HDO) selectivity was improved by suppressing decarbonylation and ring hydrogenation pathways, which was attributed to the ability of the ligands to control the binding orientation of benzyl alcohol.

The same group reported the impact of pretreatment and use of hydrophilic and hydrophobic thiolates SAMs modifiers (1-thioglycerol (TG), thiolactic acid (TLA), adamantanethiol (AT) and 1-octadecanethiol (C18)) (**Fig. 31**) over Pd/Al_2O_3 for the partial oxidation of glutaraldehyde (GA) to glutaric semialdehyde (GSA) [199]. When using catalysts coated with hydrophilic thiols such as TG and TLA, an enhancement in selectivity was observed, although conversion was affected.

S-donor ligands were also used as chiral modifiers for application in asymmetric catalysis. For instance, Lambert and co-workers reported the use of chiral sulfide ligands (**Fig. 32**) as modifiers of commercial Pd/C for applications in the enantioselective catalytic hydrogenation of isophorone [200]. Using chiral sulfide ligands that strongly bind to Pd NPs and resist displacement, they reported the first heterogeneous enantioselective catalytic hydrogenation of isophorone with ee's up to 15%. The variation in asymmetric induction across the series of ligands was correlated with the size of the alkyl group in the sulfide.

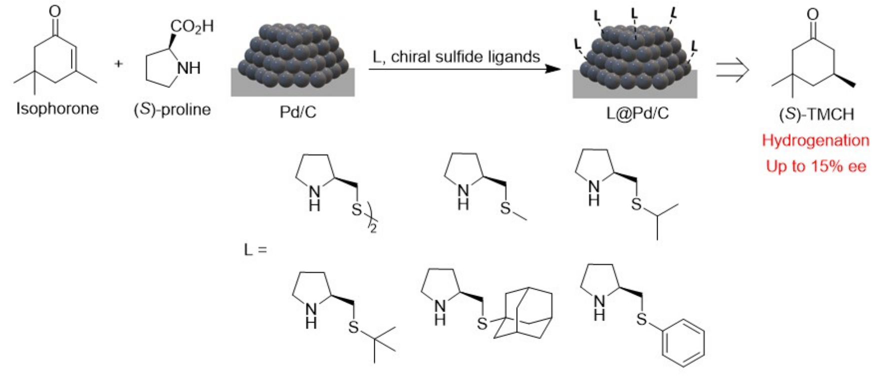

Lambert and co-workers, 2009

Fig. 32. Chiral sulfide ligands used as modifiers of commercial Pd/C for applications in the enantioselective catalytic hydrogenation of isophorone.

Another example was reported by Weng and Zaera who modified a previously synthesised Pt/Al_2O_3 catalyst with thiols (**Fig. 33**). The Pd catalyst was prepared via the formation of colloidal Pt NPs and their subsequent immobilization onto Al_2O_3. The modifiers used were 1-propanethiol, 1-hexaethiol, 1-nonanethiol, 1-hexadecanethiol and a cinchonidine-derivatized thiol [201]. First, colloidal naked MNPs were synthesized according to the literature [202] and subsequent, they were coated using the modifiers. For the preparation of the supported ones, the previously naked colloidal MNPs were dispersed in ethanol in presence of the support. They were also covered with the previously mentioned modifiers. The modification of this catalyst by thiols resulted in enhancement of both activity and selectivity in the hydrogenation of ethyl pyruvate. These heterogeneous catalysts can promote the α-keto ester hydrogenation reaction with similar enantioselectivity than the best naked supported Pt catalysts [203] without requiring the addition of cinchonidine to the reaction mixture.

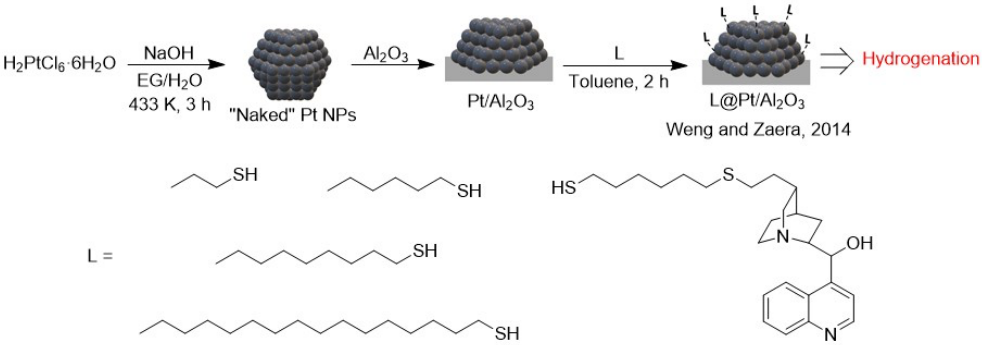

Fig. 33. Preparation of thiol-modified Pt catalysts supported onto Al_2O_3.

6. Conclusions and perspectives

This chapter highlights how the functionalization of heterogeneous catalysts by capping ligands constitutes an efficient method for the tuning of the structure and catalytic performance of supported metal nanoparticles.

The capping ligands can be introduced through several synthetic methodology according to the objectives to be reached. Introduction of these capping agents via colloidal methods, either by formation of colloids followed by deposition onto the support or by direct synthesis of the supported MNPs, can influence the size, shape and distribution of the MNPs at the support surface. Functionalization of pre-synthesized heterogeneous catalysts usually causes minor structural modifications of the nanoparticles but can enhance the catalytic performance through various effect such as alterations of the electronic properties of the surface atoms, poisoning of active sites, increase of the steric hindrance at the metal surface, etc.

The design of functionalized heterogeneous catalysts has been largely influenced by the knowledge acquired in homogeneous catalysis where precise mechanistic insights were acquired by spectroscopic investigations as well as theoretical calculations. The effects caused by the capping ligands are mainly influenced by their nature and properties such as electron donating/withdrawing abilities, steric hindrance, binding strength, etc.

Consequently, through the selection of the appropriate synthetic methodology and ligand, the activity of the catalysts can be enhanced by either modifying the electronic properties of the active phase or by increasing the relative surface area (size dependent) and/or active sites (shape dependent). The selectivity is usually influenced by the steric hindrance of the capping ligands and their ability to strongly bind the metal surface and as such, limit their mobility over the catalyst. In the case of asymmetric catalysis, this latter parameter is particularly important to condition the approach of the substrate to the active sites of the catalysts and thus provide enantio-induction. To improve the catalyst stability and allow its recycling, the synthetic strategy is key and the addition of extra ligands between each cycle is sometimes necessary to maintain the activity/selectivity of the catalysts.

The large numbers of ligands that were originally designed for homogeneous catalysis still provide a wide range of possibility for the efficient functionalization of the metal surface of heterogeneous catalysts. More recently, some of these ligands were also adapted to be introduced on the support surface and offer additional possibilities.

The specific design of ligands for heterogeneous catalysts to favor interactions with the metal surface, the support and/or with the substrates to be transformed during catalysis remains at an early stage and will probably be a focus of interest in the future.

7. References

---

1 Sau T K, Rogach A L (2010) Nonspherical Noble Metal Nanoparticles: Colloid-Chemical Synthesis and Morphology Control Adv. Mater. 22: 1781-1804.
2 You H, Yang S, Ding B, Yang H (2013) Synthesis of colloidal metal and metal alloy nanoparticles for electrochemical energy applications Chem Soc Rev 42: 2880–2904.
3 Cheong S, Watt J D, Tilley R D (2010) Shape control of platinum and palladium nanoparticles for catalysis Nanoscale, 2: 2045–2053.
4 See for instance Delgado, J A, Benkirane O, Claver C, Curulla-Ferré, Godard C (2017) Advances in the preparation of highly selective nanocatalysts for the semi-hydrogenation of alkynes using colloidal approaches Dalton Trans 46: 2381–12403.
5 Lu L, Zou S, Fang B (2021) The Critical Impacts of Ligands on Heterogeneous Nanocatalysis: A Review ACS Catal 11: 6020-6058.
6. Heuer-Jungemann A, Feliu N, Bakaimi I, Hamaly M, Alkilany A, Chakraborty I, Masod A, Casula M F, Kostopoulou A, Oh E, Susumu K, Stewart M H, Medintz I L, Stratakis E, Parak W J, Kanaras A G (2019) The role of ligands in the chemical synthesis and applications of inorganic nanoparticles Chem Rev 119:4819–4880.
7. Pujari S, Scheres L, Marcelis A T, Zuihof H, (2014) Covalent surface modification of oxide surfaces Angew Chem Int Ed 53:6322–6356
8. Jacinto M J, Kiyohara P K, Masunaga S H, Jardim R F, Rossi L M, (2008) Recoverable rhodium nanoparticles: synthesis, characterization and catalytic performance in hydrogenation reactions. Appl Catal A 338:52–57
9. Guerrero M, Costa N J S, Vono L L R, Rossi L M, Gusevskaya E V, Philippot K, (2013) Taking advantage of a terpyridine ligand for the deposition of Pd nanoparticles onto a magnetic material for selective hydrogenation reactions. J Mater Chem A 1:1441–1449
10. Choi J-Y, Hsu R S, Chen Z, (2010) Highly active porous carbon-supported nonprecious metal−n electrocatalyst for oxygen reduction reaction in PEM Fuel Cells. J Phys Chem C 114:8048–8053
11. Liu Z, Shamsuzzoha M, Ada E T, Reichert W M, Nikles D E, (2007) Synthesis and activation of Pt nanoparticles with controlled size for fuel cell electrocatalysts. J Power Sources 164:472–480
12. Peng Z, Yang H, (2009) Synthesis and oxygen reduction electrocatalytic property of Pt-on-Pd bimetallic heteronanostructures. J Am Chem Soc 131:7542–7543
13. Kim S W, Park J, Jang Y, Chung Y, Hwang S, Hyeon T, Kim Y W, (2003) Synthesis of monodisperse palladium nanoparticles. Nano Lett 3:1289–1291
14. Liu Q S, Bauer J C, Schaak R E, Lunsford J H (2008) Supported palladium nanoparticles: an efficient catalyst for the direct formation of H_2O_2 from H_2 and O_2. Angew Chem Int Ed 47:6221–6224
15. Ramírez-Meneses E, Domínguez-Crespo M A, Montiel-Palma V, Chávez-Herrera V H, Gómez E, Hernández-Tapia G, (2009) Electrochemical characterization of platinum nanoparticles stabilized by amines. J of Alloys Compd 483:573–577
16. Miyabayashi K, Nishihara H, Miyake M, (2014) Platinum nanoparticles modified with alkylamine derivatives as an active and stable catalyst for oxygen reduction reaction. Langmuir 30:2936–2942
17. Brust M, Walker M, Bethell D, Schiffrin D, Whyman R, (1994) Synthesis of thiol derivatised gold nanoparticles in a two-phase liquid-liquid system. J Chem Soc Chem Commun 801−802
18. Miyabayashi K, Miyake M, (2017) Platinum nanoparticles modified with perfluorinated alkylamines as a model cathode catalyst for fuel cells. Electroanalysis 29:898–906
19. Ung D, Cossairt B M, (2019) Effect of surface ligands on CoP for the hydrogen evolution reaction. ACS Appl Energy Mater 2:1642–1645
20. Xia B Y, Ng W T, Wu H B, Wang X, Lou X W, (2012) Self-supported interconnected Pt nanoassemblies as highly stable electrocatalysts for low-temperature fuel cells. Angew Chem 124:7325–7328
21. Xu Z, Shen C, Hou Y, Gao H, Sun S, (2009) Oleylamine as both reducing agent and stabilizer in a facile synthesis of magnetite nanoparticles. Chem Mater 21:1778–1780
22. Tzitzios V, Niarchos D, Gjoka M, Boukos N, Petridis D, (2005) Synthesis and characterization of 3D CoPt nanostructures. J Am Chem Soc 127:13756–13757
23. Lim B, Xia Y, (2011) Metal nanocrystals with highly branched morphologies. Angew Chem Int Ed 50:76–85
24. Park K H, Jang K, Kim H J, Son S U, (2007) Near-monodisperse tetrahedral rhodium nanoparticles on charcoal: the shape-dependent catalytic hydrogenation of arenes. Angew Chem Int Ed 46:1152–1155

---

25. Borchert H, Fenske D, Kolny-Olesiak J, Parisi J, Al-Shamery K, Bäumer M, (2007) Ligand-capped Pt nanocrystals as oxide-supported catalysts: FTIR spectroscopic investigations of the adsorption and oxidation of CO. Angew Chem Int Ed 46:2923–2926
26. Sonström P, Halbach B, Djakpou S T, Ritz B, Ahrenstorf K, Grathwohl G, Weller H, Bäumer M, (2011) Foam, fleece and honeycomb: catalytically active coatings from colloidally prepared nanoparticles. Catal Sci Technol 1:830–838
27. Sonström P, Arndt D, Wang X, Zielasek V, Bäumer M, (2011) Ligand capping of colloidally synthesized nanoparticles—a way to tune metal–support interactions in heterogeneous gas-phase catalysis. Angew Chem Int Ed 50:3888–3891
28. Wang X, Sonström P, Arndt D, Stöver J, Zielasek V, Borchert H, Thiel K, Al-Shamery K, Bäumer M, (2011) Heterogeneous catalysis with supported platinum colloids: a systematic study of the interplay between support and functional ligands. J Catal 278:143–152
29. Chen T, Xu Z, (2018) Immobilization of small-molecule ligands containing secondary or tertiary amine groups onto TiO_2-supported Ru catalysts driven by the hydrophobic effect. ChemistrySelect 3:6421–6425
30. Jana N R, Peng X, (2003) Single-phase and gram-scale routes toward nearly monodisperse Au and other noble metal nanocrystals. J Am Chem Soc 125:14280–14281
31. Altmann L, Wang X, Stçver J, Klink M, Zielasek V, Thiel K, Kolny-Olesiak J, Al-Shamery K, Borchert H, Parisi J, Bäumer M, (2013) Impact of organic ligands on the structure and hydrogenation performance of colloidally prepared bimetallic PtSn nanoparticles. ChemCatChem 5:1803–1810
32. Costa N J S, Guerrero M, Collière V, Teixeira-Neto E, Landers R, Philippot K, Rossi L R, (2014) Organometallic preparation of Ni, Pd, and NiPd nanoparticles for the design of supported nanocatalysts. ACS Catal 4:1735–1742
33. Zaramello L, Albuquerque B L, Domingos J B, Philippot K, (2017) Kinetic investigation into the chemoselective hydrogenation of α,β-unsaturated carbonyl compounds catalyzed by Ni(0) nanoparticles. Dalton Trans 46:5082–5090
34. Zheng G, Kaefer K, Mourdikoudis S, Polavarapu L, Vaz B, Cartmell S E, Bouleghlimat A, Buurma N J, Yate L, de Lera A R, Liz-Marzán L M, Pastoriza-Santos I, Pérez-Juste J, (2015) Palladium nanoparticle-loaded cellulose paper: a highly efficient, robust, and recyclable self-assembled composite catalytic system. J Phys Chem Lett 6:230–238
35. Sato R, Kanehara M, Teranishi T, (2011) Homoepitaxial size control and large-scale synthesis of highly monodisperse amine-protected palladium nanoparticles. Small 7:469–473
36. Altmann L, Wang X, Borchert H, Kolny-Olesiak J, Zielasek V, Parisi J, Kunz S, Bäumer M, (2015) Influence of Sn content on the hydrogenation of crotonaldehyde catalysed by colloidally prepared PtSn nanoparticles. Phys Chem Chem Phys 17:28186–28192
37. Luo W, Cheng W, Hu M, Wang Q, Cheng X, Zhang Y, Wang Y, Gao D, Bi J, Fan G, (2019) Ultrahigh catalytic activity of L-proline-functionalized Rh nanoparticles for methanolysis of ammonia borane. ChemSusChem 12:535–541
38. Schmid G, Harms M, Malm J-O, Bovin J-O, Ruitenbeck J V, Zandbergen H W, Fu W T, (1993) Ligand-stabilized giant palladium clusters: promising candidates in heterogeneous catalysis. J Am Chem Soc 115:2046–2048
39. Schmid G, Emde S, Maihack V, Meyer-Zaika W, Peschel S, (1996) Synthesis and catalytic properties of large ligand stabilized palladium clusters. J Mol Catal A: Chem 107:95–104
40. Schmid G, Maihack V, Lantermann F, Peschel S, (1996) Ligand-stabilized metal clusters and colloids: properties and applications. J Chem Soc Dalton Trans 589–595
41. Schmid G, West H, Mehles H, Lehnert A, (1997) Hydrosilation reactions catalyzed by supported bimetallic colloids. Inorg Chem 36:891–895
42. (a) Turkevich J, Stevenson P C, Hillier J, (1951) A study of the nucleation and growth processes in the synthesis of colloidal gold. Discuss Faraday Soc 11:55–75; (b) Turkevich J, Kim G, (1970) Palladium: preparation and catalytic properties of particles of uniform size. Science 169:873–879; (c) Schmid G, Lehnert A, (1989) The complexation of gold colloids. Angew Chem Int Ed Engl 28:780–781; (d) Schmid G, Lehnerf A, Malm J-O, Bovin J-O, (1991) Ligand-stabilized bimetallic colloids identified by HRTEM and EDX. Angew Chem Int Ed Engl 30:874–876
43. Schmid G, West H, Malm J-O, Bovin J-O, Grenthe C, (1996) Catalytic properties of layered gold–palladium colloids. Chem Eur J 2:1099–1103
44. Jahjah M, Kihn Y, Teuma E, Gómez M, (2010) Ruthenium nanoparticles supported on multi-walled carbon nanotubes: highly effective catalytic system for hydrogenation processes. J Mol Catal A: Chem 332:106–112

45. Favier I, Massou S, Teuma E, Philippot K, Chaudret B, Gómez M, (2008) A new and specific mode of stabilization of metallic nanoparticles. Chem Commun 3296–3298

46. Rodríguez-Pérez L, Pradel C, Serp P, Gómez M, Teuma E, (2011) Supported ionic liquid phase containing palladium nanoparticles on functionalized multiwalled carbon nanotubes: catalytic materials for sequential Heck coupling/hydrogenation process. ChemCatChem 3:749–754

47. Romero N, Guerra R B, Gil L, Drouet S, Salmeron-Sánchez I, Illa O, Philippot K, Natali M, García-Antón J, Sala X, (2020) TiO_2-mediated visible-light-driven hydrogen evolution by ligand-capped Ru nanoparticles. Sustain Energy Fuels 4:4170–4178

48. Creus J, Drouet S, Suriñach , Lecante P, Collière V, Poteau R, Philippot K, García-Antón J, Sala X, (2018) Ligand-capped Ru nanoparticles as efficient electrocatalyst for the hydrogen evolution reaction. ACS Catal 8:11094–11102

49. Bönnemann H, Braun G A, (1997) Enantioselectivity control with metal colloids as catalysts. Chem Eur J 3:1200–1202

50. Wu J, Zhang J, Peng Z, Yang S, Wagner F T, Yang H, (2010) Truncated octahedral Pt_3Ni oxygen reduction reaction electrocatalysts. J Am Chem Soc 132:4984–4985

51. (a) Mullen T J, Dameron A A, Saavedra H M, Williams M E, Weiss P S, (2007) Dynamics of solution displacement in 1-adamantanethiolate self-assembled monolayers. J Phys Chem C 111:6740–6746; (b) Maksimuk S, Teng X, Yang H, (2007) Roles of twin defects in the formation of platinum multipod nanocrystals. J Phys Chem C 111:14312–14319

52. Wu J, Qi L, You H, Gross A, Li J, Yang H, (2012) Icosahedral platinum alloy nanocrystals with enhanced electrocatalytic activities. J Am Chem Soc 134:11880–11883

53. (a) Wu J B, Gross A, Yang H, (2011) Shape and composition-controlled platinum alloy nanocrystals using carbon monoxide as reducing agent. Nano Lett 11:798–802; (b) Kang Y, Ye X, Murray C B, (2010) Size- and shape-selective synthesis of metal nanocrystals and nanowires using CO as a reducing agent. Angew Chem Int Ed 49:6156–6159

54. (a) Wu B H, Zheng N F, Fu G, (2011) Small molecules control the formation of Pt nanocrystals: a key role of carbon monoxide in the synthesis of Pt nanocubes. Chem Commun 47:1039–1041; (b) Schauermann S, Hoffmann J, Johanek V, Hartmann J, Libuda J, Freund H J, (2002) Catalytic activity and poisoning of specific sites on supported metal nanoparticles. Angew Chem Int Ed 41:2532–2535; (c) Eichler A, (2002) CO oxidation on transition metal surfaces: reaction rates from first principles. Surf Sci 498:314–320; (d) Somorjai G A, Li Y, Introduction to surface chemistry and catalysis, 2nd ed.; John Wiley & Sons: Hoboken, NJ, 2010

55. Gan L, Heggen M, Rudi S, Strasser P, (2012) Core−shell compositional fine structures of dealloyed Pt_xNi_{1-x} nanoparticles and their impact on oxygen reduction catalysis. Nano Lett 12:5423–5430

56. Ahrenstorf K, Albrecht O, Heller H, Kornowski A, Görlitz D, Weller H, (2007) Colloidal Synthesis of Ni_xPt_{1-x} Nanoparticles with Tuneable Composition and Size. Small 3:271–274

57. Jürgens B, Borchert H, Ahrenstorf K, Sonström P, Pretorius A, Schowalter M, Gries K, Zielasek V, Rosenauer A, Weller H, Bäumer M, (2008) Colloidally prepared nanoparticles for the synthesis of structurally well-defined and highly active heterogeneous catalysts. Angew Chem Int Ed 47:8946–8949

58. Yin Z, Zhang Y, Chen K, Li J, Li W, Tang P, Zhao H, Zhu Q, Bao X, Ma D, (2014) Monodispersed bimetallic PdAg nanoparticles with twinned structures: formation and enhancement for the methanol oxidation. Sci Rep 4:4288

59. Yin Z, Ma D, Bao X H, (2010) Emulsion-assisted synthesis of monodisperse binary metal nanoparticles. Chem Commun 46:1344–1346

60. Winnischofer H, Rocha T C,Nunes W C, Socolovsky L M, Knobel M, Zanchet D, (2008) Chemical synthesis and structural characterization of highly disordered Ni colloidal nanoparticles. ACS Nano 2:1313–1319

61. Yang J, Deivaraj T C, Too H P, Lee J Y, (2004) Acetate stabilization of metal nanoparticles and its role in the preparation of metal nanoparticles in ethylene glycol. Langmuir 20:4241–4245

62. Li D, Komarneni S, (2006) Microwave-assisted polyol process for synthesis of Ni nanoparticles. J Am Ceram Soc 89:1510–1517

63. Rinaldi R, de Melo Porcari A, Rocha T C R, Cassinelli W H C, Ribeiro R U, Bueno J M C, Zanchet D, (2009) Construction of heterogeneous Ni catalysts from supports and colloidal nanoparticles – A challenging puzzle. J Mol Catal A: Chem 301:11–17

64. Yi D, Min Y, Muzzi B, Marty A, Romana I, Fazzini P-F, Blon T, Viau G, Serp P, Soulantica K, (2022) Epsilon cobalt nanoparticles as highly performant catalysts in cinnamaldehyde selective hydrogenation. ACS Appl Nano Mater 5:5498–5507

---

65. Liakakos N, Cormary B, Li X, Lecante P, Respaud M, Maron L, Falqui A, Genovese A, Vendier L, Koïnis S, Chaudret B, Soulantica K, (2012) The big impact of a small detail: cobalt nanocrystal polymorphism as a result of precursor addition rate during stock solution preparation. J Am Chem Soc 134:17922–17931

66. Cormary B, Li T, Liakakos N, Peres L, Fazzini P-F, Blon T, Respaud M, Kropf A J, Chaudret B, Miller J T, Mader E A, Soulantica K, (2016) Concerted growth and ordering of cobalt nanorod arrays as revealed by tandem in situ SAXS-XAS studies. J Am Chem Soc 138:8422–8431

67. Metin Ö, Mazumder V, Özkar S, Sun S, (2010) Monodisperse nickel nanoparticles and their catalysis in hydrolytic dehydrogenation of ammonia borane. J Am Chem Soc 132:1468–1469

68. Chung Y-H, Kim S J, Chung D Y, Park H Y, Sung Y-E, Yoo S J, Jang J H, (2015) Third-body effects of native surfactants on Pt nanoparticle electrocatalysts in proton exchange fuel cells. Chem Commun 51:2968–2971

69. Peres L, Axet M R, Yi D, Serp P, Soulantica K, (2020) Selective hydrogenation of cinnamaldehyde by unsupported and few layer graphene supported platinum concave nanocubes exposing {110} facets stabilized by a long-chain amine. Catal Today 357:166–175

70. Peres L, Yi D, Bustos-Rodriguez S, Marcelot C, Pierrot A, Fazzini P F, Florea I, Arenal R, Lacroix L M, Warot-Fonrose B, Blon T, Soulantica K, (2018) Shape selection through epitaxy of supported platinum nanocrystals. Nanoscale 10:22730–22736

71. Buil M L, Esteruelas M A, Niembro S, Oliván M, Orzechowski L, Pelayo C, Vallribera A, (2010) Organometallics 29:4375–4383

72. Qi S-C, Zhang L, Einaga H, Kudo S, Norinaga K, Jun-ichiro Hayashi, (2017) Nano-sized nickel catalyst for deep hydrogenation of lignin monomers and first-principles insight into the catalyst preparation. J Mater Chem A 5:3948–3965

73. Castillejos E, Debouttière P-J, Roiban L, Solhy A, Martinez V, Kihn Y, Ersen O, Philippot K, Chaudret B, Serp P, (2009) An efficient strategy to drive nanoparticles into carbon nanotubes and the remarkable effect of confinement on their catalytic performance. Angew Chem Int Ed 48:2529–2533

74. Harmel J, Berliet A, Dembélé K, Marcelot C, Gay A-S, Ersen O, Maury S, Fécant A, Chaudret B, Serp P, Soulantica K, (2018) A seed-mediated approach for the preparation of modified heterogeneous catalysts. ChemCatChem 10:1614–1619

75. Xia Y, Gilroy K D, Peng H-C, Xia X, (2017) Seed-mediated growth of colloidal metal nanocrystals. Angew Chem Int Ed 56:60–95

76. Campisi S, Schiavoni M, Chan-Thaw C E, Villa A, (2016) Untangling the role of the capping agent in nanocatalysis: recent advances and perspectives. Catalysts 6:185

77. Harmel J, Peres L, Estrader M, Berliet A, Maury S, Fécant A, Chaudret B, Serp P, Soulantica K, (2018) *hcp*-Co nanowires grown on metallic foams as catalysts for Fischer–Tropsch synthesis. Angew Chem Int Ed 57:10579–10583

78. Cormary B, Dumestre F, Liakakos N, Soulantica K, Chaudret B, (2013) Organometallic precursors of nano-objects, a critical view. Dalton Trans 42:12546–12553

79. (a) Dumestre F, Chaudret B, Amiens C, Fromen M-C, Casanove M-J, Renaud P, Zurcher P, (2002) Shape control of thermodynamically stable cobalt nanorods through organometallic chemistry. Angew Chem Int Ed 41:4286–4289; (b) Liakakos N, Cormary B, Li X, Lecante P, Respaud M, Maron L, Falqui A, Genovese A, Vendier L, Koïnis S, Chaudret B, Soulantica K, (2012) The big impact of a small detail: cobalt nanocrystal polymorphism as a result of precursor addition rate during stock solution preparation. J Am Chem Soc 134:17922–17931; (c) Cormary B, Li T, Liakakos N, Peres L, Fazzini P-F, Blon T, Respaud M, Kropf A J, Chaudret B, Miller J T, Mader E A, Soulantica K, (2016) Concerted growth and ordering of cobalt nanorod arrays as revealed by tandem in situ SAXS-XAS studies. J Am Chem Soc, 138:8422–8431

80. Boitiaux J P, Cosyns J, Vasudevan S, (1985) Hydrogenation of highly unsaturated hydrocarbons over highly dispersed Pd catalyst. Part II: ligand effect of piperidine. Appl Catal 15:317–326

81. Boitiaux J P, Cosyns J, Vasudevan S, (1983) Hydrogenation of highly unsaturated hydrocarbons over highly dispersed palladium catalyst. Part I: behaviour of small metal particles. Appl Catal 6:41–51

82. Boitiaux J P, Cosyns J, Vasudevan S, (1982) Proc 3rd Int Symp on the Scientific Bases for the Preparation of Heterogeneous Catalysts, Belgium, Elsevier.

83. Chung Y-H, Chung D Y, Jung N, Sung Y-E, (2013) Tailoring the electronic structure of nanoelectrocatalysts induced by a surface-capping organic molecule for the oxygen reduction reaction. J Phys Chem Lett 4:1304–1309

84. Wang Y, Ren J, Deng K, Gui L, Tang Y, (2000) Preparation of tractable platinum, rhodium, and ruthenium nanoclusters with small particle size in organic media. Chem Mater 12:1622–1627

---

85. Munnik P, de Jongh P E, de Jong K P, (2015) Recent developments in the synthesis of supported catalysts. Chem Rev 115:6687–6718

86. Liu J, Sun M, Lin Q, Liu S, Xu H, Chen Y, (2019) Promotional effects of ethylenediamine on the low-temperature catalytic activity of selective catalytic oxidation of ammonia over Pt/$SiAlO_x$: States and particle sizes of Pt. Appl Surf Sci 481:1344–1351

87. Tungler A, Máthé T, Petró J, in: Proceedings of the Second Czechoslovakian Conf on Het Cat, Bechyne, 1985

88. Tungler A, Kajtár M, Máthé T, Petró J, in: Proceedings of the Fourth Belgian-Hungarian Conf on Catalysis, Herbeaumont, 1987

89. Tungler A, Kajtár J, Máthé T, Tóth T, Fogassy E, Petró J, (1989) Enantioselective hydrogenation of α-β-unsaturated ketones. Catal Today 5:159–171

90. Li S, Chen C, Zhan E, Liu S-B, Shen W, (2009) Chirality inversion in enantioselective hydrogenation of isophorone over Pd/MgO catalysts in the presence of (*S*)-proline: Effect of Pd particle size. J Mol Catal A: Chem 304:88–94

91. Győrffy N, Tungler A, Fodor M, (2010) Stereodifferentiation in heterogeneous catalytic hydrogenation. Kinetic resolution and asymmetric hydrogenation in the presence of (*S*)-proline: catalyst-dependent processes. J Catal 270:2–8

92. Künzle N, Hess R, Mallat T, Baiker A, (1999) Continuous enantioselective hydrogenation of activated ketones. J Catal 186:239–241

93. Blaser H U, Jalett H P, Lottenbach W, Studer M, (2000) Heterogeneous enantioselective hydrogenation of ethyl pyruvate catalyzed by cinchona-modified Pt catalysts: effect of modifier structure. J Am Chem Soc 122:12675–12682

94. Panella B, Vargas A, Baiker A, (2009) Magnetically separable Pt catalyst for asymmetric hydrogenation. J Catal 261:88–93

95. Sugimura T, Ogawa H, (2010) Acceleration of enantioselective hydrogenation of olefins over Pd/C by cinchonidine as a chiral codifier. Comparison with cinchonine, pseudoenantiomer. Chem Lett 39:232–233

96. Diezi S, Ferri D, Vargas A, Mallat T, Baiker A, (2006) The origin of chemo- and enantioselectivity in the hydrogenation of diketones on platinum. J Am Chem Soc 128:4048–4057

97. García-Suárez E J, Tristany M, García A B, Collière V, Philippot K, (2012) Carbon-supported Ru and Pd nanoparticles: efficient and recyclable catalysts for the aerobic oxidation of benzyl alcohol in water. Microporous Mesoporous Mater 153:155–162

98. Castillejos E, Debouttière P-J, Roiban L, Solhy A, Martinez V, Kihn Y, Ersen O, Philippot K, Chaudret B, Serp P, (2009) An efficient strategy to drive nanoparticles into carbon nanotubes and the remarkable effect of confinement on their catalytic performance. Angew Chem Int Ed 48:2529–2533

99. Favier I, Massou S, Teuma E, Philippot K, Chaudret B, Gómez M, (2008) A new and specific mode of stabilization of metallic nanoparticlesw. Chem Commun 28:3296–3298

100. Ramirez E, Jansat S, Philippot K, Lecante P, Gómez M, Masdeu A, Chaudret B, (2004) Influence of organic ligands on the stabilization of palladium nanoparticles. J Organomet Chem 689:4601–4610

101. García-Suárez E J, Balu A M, Tristany M, García A B, Philippot K, Luque R, (2012) Versatile dual hydrogenation–oxidation nanocatalysts for the aqueous transformation of biomass-derived platform molecules. Green Chem 14:1434–1439

102. Jeong H, Kim C, Yang S, Lee H, (2016) Selective hydrogenation of furanic aldehydes using Ni nanoparticle catalysts capped with organic molecules. J Catal 344:609–615

103. Carenco S, Boissiere C, Nicole L, Sanchez C, Le Floch P, Mezailles N, (2010) Controlled design of size-tunable monodisperse nickel nanoparticles. Chem Mater 22:1340–1349

104. Castillejos E, Jahjah M, Favier I, Orejón A, Pradel C, Teuma E, Masdeu-Bultó A M, Serp P, Gómez M, (2012) Synthesis of platinum–ruthenium nanoparticles under supercritical CO_2 and their confinement in carbon nanotubes: hydrogenation applications. ChemCatChem 4:118–122

105. Ruiz D, Mella C, Fierro J L G, Reyes P, (2012) Silica supported rhodium metal nanoparticles stabilized with (-)-DIOP. Effect of ligand concentration and metal loading on the enantioselective hydrogentation of ketones. J Chil Chem Soc 57:1394–1399

106. Mella C, Ávila M, Sánchez A, Marzialetti T, Reyes P, Ruiz D, (2013) Chiral Rh/SiO_2 catalysts for enantioselective hydrogenation reactions. The role of (*S*,*S*)-DIPAMP as chiral modifier and stabilizer on metallic nanoparticles synthesis. J Chil Chem Soc 58:2125–2130

107. Ruiz D, Mäki-Arvela P, Aho A, Chimentão R, Claver C, Godard C, Fierro J L G, Murzin D Y, (2019) Immobilized chiral rhodium nanoparticles stabilized by chiral P-ligands as efficient catalysts for the enantioselective hydrogenation of 1-phenyl-1,2-propanedione. Mol Catal 477:110551

109. Han D, Li X, Zhang H, Liu Z, Hu G, Li C, (2008) Asymmetric hydroformylation of olefins catalyzed by rhodium nanoparticles chirally stabilized with (*R*)-BINAP ligand. J Mol Catal A: Chem 283:15–22

110. Jiang H-y, Yang C-f, Li C, Fu H-y, Chen H, Li R-x, Li X-j, (2008) Heterogeneous enantioselective hydrogenation of aromatic ketones catalyzed by cinchona- and phosphine-modified iridium catalysts. Angew Chem Int Ed 47:9240–9244

111. Jiang H-y, Sun B, Zheng X-x, Chen H, (2012) Heterogeneous selective hydrogenation of *trans*-4-phenyl-3-butene-2-one to allylic alcohol over modified Ir/SiO_2 catalyst. App Catal A: Gen 421–422:86–90

112. Castelbou J L, Szeto K C, Barakat W, Merle N, Godard C, Taoufik M, Claver C, (2017) Chem Commun 53:3261–3264

113. Sánchez-Resa D, Delgado J A, Fernández-Martínez M D, Didelot C, De Mallmann A, Szeto K C, Taoufik M, Claver C, Godard C, (2021) Pd, Cu and bimetallic PdCu NPs supported on CNTs and phosphine-functionalized silica: one-pot preparation, characterization and testing in the semi-hydrogenation of alkynes. Eur J Inorg Chem 4970–4978

114. Montiel, L, Delgado J A, Novell, M, Andrade, F J, Claver, C, Blondeau, P, Godard, C, (2016) A Simple and Versatile Approach for the Fabrication of Paper-Based Nanocatalysts: Low Cost, Easy Handling, and Catalyst Recovery. ChemCatChem 3041–3044.

115. Fernández-Martínez M D, Godard C, (2023) Hydrogenation of CO_2 into Formates by Ligand-Capped Palladium Heterogeneous Catalysts. ChemCatChem e202201408

116. Tang B, Xiong W, Liu D-R, Jia Y, Wang J-B, Chen H, Li X-J, (2008) Asymmetric hydrogenation of aromatic ketones catalyzed by (1*S*,2*S*)-DPEN-modified Ru-PPh_3/γ-Al_2O_3 catalyst. Tetrahedron: Asymmetry 19:1397–1401

117. Coronado J M, Coloma F, Anderson J A, (2000) Styrene hydroformylation over modified Rh/$SiO_2 \cdot Al_2O_3$ catalysts. J Molecular Catal A: Chem 154:143–154

118. Yan L, Ding Y J, Zhu H J, Xiong J M, Wang T, Pan Z D, Lin L W, (2005) Ligand modified real heterogeneous catalysts for fixed-bed hydroformylation of propylene. J Mol Catal A: Chem 234:1–7

119. Li X, Ding Y, Jiao G, Li J, Yan L, Zhu H, (2008) Hydroformylation of methyl-3-pentenoate over a phosphite ligand modified Rh/SiO_2 catalyst, J Nat Gas Chem 17:351–354

120. Mori K, Kondo Y, Yamashita H, (2009) Synthesis and characterization of FePd magnetic nanoparticles modified with chiral BINAP ligand as a recoverable catalyst vehicle for the asymmetric coupling reaction. Phys Chem Chem Phys 11:8949–8954

121. Felpin F-X, Landais Y, (2005) Practical Pd/C-mediated allylic substitution in water. J Org Chem 70:6441–6446

122. Reimann S, Mallat T, Baiker A, (2007) Enantioselective allylic substitution on Pd/Al_2O_3 modified by chiral diphosphines. J Catal 252:30–38

123. Reimann S, Mallat T, Baiker A, (2008) A new, efficient heterogeneous Pd catalyst for enantioselective allylic substitution. J Catal 254:79–83

124. Reimann S, Grunwaldt J-D, Mallat T, Baiker A, (2010) Asymmetric C-C Bond-formation reaction with Pd: how to favor heterogeneous or homogeneous catalysis? Chem Eur J 16:9658–9668

125. Park K H, Chung Y K, (2005) Immobilized Co/Rh heterobimetallic nanoparticle-catalyzed Pauson–Khand-type reaction. Adv Synth Catal 347:854–866

126. Cheng H, Hao J, Wang H, Xi C, Meng X, Cai S, Zhao F, (2007) (*R*,*R*)-DPEN-modified Ru/γ-Al_2O_3—An efficient heterogeneous catalyst for enantioselective hydrogenation of acetophenone. J Mol Catal A: Chem 278:6–11

127. Wang H, Huang Y, Wang X, Cui X, Shi F, (2020) Supported Ni nanoparticles with a phosphine ligand as an efficient heterogeneous non-noble metal catalytic system for regioselective hydrosilylation of alkynes. Org Biomol Chem 18, 7554–7558

128. McKenna F-M, Wells R P K, Anderson J A, (2011) Enhanced selectivity in acetylene hydrogenation by ligand modified Pd/TiO_2 catalysts. Chem Commun 47:2351–2353

129. McCue A J, McKenna F-M, Anderson J A, (2015) Triphenylphosphine: a ligand for heterogeneous catalysis too? Selectivity enhancement in acetylene hydrogenation over modified Pd/TiO_2 catalyst. Catal Sci Technol 5:2449–2459

130. Hu G, Feng Z, Han D, Li J, Jia G, Shi J, Li C, (2007) Charge transfer between triphenyl phosphine and colloidal silver: a SERS study combined with DFT calculations. J Phys Chem C 111:8632–8637

131. Sizova O V, Varshavskii Y S, Skripnikov L V, (2007) Quantum-chemical study of donor-acceptor interactions in rhodium(I) carbonyl carboxylate complexes with phosphine ligands. Russ J Coord Chem 33:313–322

132. Strozier R W, Caramella P, Houk K N, (1979) Influence of molecular distortions upon reactivity and stereochemistry in nucleophilic additions to acetylenes. J Am Chem Soc 101:1340–1343

133. Ballesteros-Soberanas J, Leyva-Pérez A, (2023) Electron-poor phosphines enable the selective semihydrogenation reaction of alkynes with Pd on carbon catalysts. J Phys Chem Lett 14:965–970

134. Han D, Li X, Zhang H, Liu Z, Li J, Li C, (2006) Heterogeneous asymmetric hydroformylation of olefins on chirally modified Rh/SiO_2 catalysts. J Catal 243:318–328

135. Korzec M, Bartczak P, Niemczyk A, Szade J, Kapkowski M, Zenderowska P, Balin K, Lelątko J, Polanski J, (2014) Bimetallic nano-Pd/PdO/Cu system as a highly effective catalyst for the Sonogashira reaction. J Catal 313:1–8

136. Tukacs J M, Jones R V, Darvas F, Dibó G, Lezsák G, Mika L T, (2013) Synthesis of γ-valerolactone using a continuous-flow reactor. RSC Adv 3:16283–16287

137. Chatterjee A, Jensen V R, (2017) A heterogeneous catalyst for the transformation of fatty acids to α-olefins. ACS Catal 7:2543–2547

138. Cui H-Z, Zhang Z-M, Zhang H, Reheman A, Hong X, Zhan B, Zhang J, Hou X-F, (2021) Mesocellular silica foams supported size-controlled Pd nanoparticles for racemic and asymmetric iodomethyl dihydrobenzofuran synthesis, Microporous Mesoporous Mater 322:111157

139. Guo M, Li H, Ren Y, Ren X, Yang Q, Li C, (2018) Improving catalytic hydrogenation performance of Pd nanoparticles by electronic modulation using phosphine ligands. ACS Catal 8:6476–6485

140. Lu Y D, Wang Y H, Jin Z L, (2010) Rh nanoparticles stabilized by PEG-substituted triphenyl-phosphine: A highly active and recyclable catalyst for aqueous biphasic hydrogenation of benzene. Chin Chem Lett 21:1067–1070

141. Jayakumar S, Modak A, Guo M, Li H, Hu X, Yang Q, (2017) Ultrasmall platinum stabilized on triphenylphosphine-modified silica for chemoselective hydrogenation. Chem Eur J 23:7791–7797

142. Ren X, Guo M, Li H, Li C, Yu L, Liu J, Yang Q, (2019) Microenvironment engineering of ruthenium nanoparticles incorporated into silica nanoreactors for enhanced hydrogenations. Angew Chem Int Ed 58:14483–14488

143. Lei Y, Chen Z, Lan G, Wang R, Zhou X-Y, (2020) Pd nanoparticles stabilized with phosphine functionalized porous ionic polymer for efficient catalytic hydrogenation of nitroarenes in water, New J Chem 44:3681–3689

144. Wang H, Fiore A M, Fliedel C, Manoury E, Philippot K, Dell'Anna M M, Mastrorilli P, Poli R, (2021) Rhodium nanoparticles inside well-defined unimolecular amphiphilic polymeric nanoreactors: synthesis and biphasic hydrogenation catalysis. Nanoscale Adv 3:2554–2566

145. Doherty S, Knight J G, Backhouse T, Tran T S T, Paterson R, Stahl F, Alharbi H Y, Chamberlain T W, Bourne R A, Stones R, Griffiths A, White J P, Aslam Z, Hardare C, Daly H, Hart J, Temperton R H, O'Shead J N, Rees N H, (2022) Highly efficient and selective aqueous phase hydrogenation of aryl ketones, aldehydes, furfural and levulinic acid and its ethyl ester catalyzed by phosphine oxide-decorated polymer immobilized ionic liquid-stabilized ruthenium nanoparticles. Catal Sci Technol 12:3549–3567

146. Costa N J S, Kiyohara P K, Monteiro A L, Coppel Y, Philippot K, Rossi L M, (2010) A single-step procedure for the preparation of palladium nanoparticles and a phosphine-functionalized support as catalyst for Suzuki cross-coupling reactions. J Catal 276:382–389

147. Rossi L M, Nangoi I M, Costa N J S, (2009) Ligand-assisted preparation of palladium supported nanoparticles: a step toward size control. Inorg Chem 48:4640

148. Cai X, Nie J, Yang G, Wang F, Ma C, Lu C, Chen Z, (2019) Phosphorus-rich network polymer supported ruthenium nanoparticles for nitroarene reduction. Mater Lett 240:80–83

149. Tegeder P, Freitag M, Chepiga K M, Muratsugu S, Möller N, Lamping S, Tada M, Glorius F, Ravoo B J, (2018) N-Heterocyclic Carbene-modified Au–Pd alloy nanoparticles and their application as biomimetic and heterogeneous catalysts. Chem Eur J 24:18682–18688

150. Ranganath K V S, Kloesges J, Schäfer A H, Glorius F, (2010) Asymmetric nanocatalysis: N-heterocyclic carbenes as chiral modifiers of Fe_3O_4/Pd nanoparticles. Angew Chem Int Ed 49:7786–7789

151. Richter C, Schaepe K, Glorius F, Ravoo B J, (2014) Tailor-made N-heterocyclic carbenes for nanoparticle stabilization. Chem Commun 50:3204–3207

152. Ferry A, Schaepe K, Tegeder P, Richter C, Chepiga K M, Ravoo B J, Glorius F, (2015) Negatively charged N-Heterocyclic Carbene-stabilized Pd and Au nanoparticles and efficient catalysis in water. ACS Catal 5:5414–5420

153. Tegeder P, Marelli M, Freitag M, Polito L, Lamping S, Psaro R, Glorius F, Ravoo B J, Evangelisti C, (2018) Metal vapor synthesis of ultrasmall Pd nanoparticles functionalized with N-heterocyclic carbenes. Dalton Trans 47:12647–1265

154. Díaz de los Bernardos M, Pérez-Rodríguez S, Gual A, Claver C, Godard C, (2017) Facile synthesis of NHC-stabilized Ni nanoparticles and their catalytic application in the *Z*-selective hydrogenation of alkynes. Chem Commun 53:7894–7897

155. Lomelí-Rosales D A, Delgado J A, Díaz de los Bernardos M, Pérez-Rodríguez S, Gual A, Claver C, Godard C, (2019) A general one-pot methodology for the preparation of mono- and bimetallic nanoparticles supported on carbon nanotubes: application in the semi-hydrogenation of alkynes and acetylene. Chem Eur J 25:8321–8331

156. Mollar-Cuni A, Ventura-Espinosa D, Martín S, Mayoral Á, Borja P, Mata J A, (2018) Stabilization of nanoparticles produced by hydrogenation of palladium−N-Heterocyclic Carbene complexes on the surface of graphene and implications in catalysis. ACS Omega 3:15217–15228

157. Mollar-Cuni A, Martín S, Guisado-Barrios G, Mata J A, (2023) Dual role of graphene as support of ligand-stabilized palladium nanoparticles and carbocatalyst for (de)hydrogenation of N-heterocycles. Carbon 206:314–324

158. Oberhauser W, Evangelisti C, Liscio A, Kovtun A, Cao Y, Vizza F, (2018) Glycerol to lactic acid conversion by NHC-stabilized iridium Nanoparticles. J Catal 368:298–305

159. Azad M, Rostamizadeh S, Nouri F, Estiri H, Fadakar Y, (2019) Pd nanoparticles at N-Heterocyclic Carbene at ZIF-8 as an ultrafine, robust and sustainable heterogeneous system for Suzuki-Miyaura cross coupling processes. Mat Lett 236:757–760

160. Zhang L, Wei Z, Thanneeru S, Meng M, Kruzyk M, Ung G, Liu B, He J, (2019) Polymer solution to prevent nanoclustering and improve the selectivity of metal nanoparticles for electrocatalytic CO$_2$ reduction. Angew Chem Int Ed 58:15834–15840

161. Palazzolo A, Naret T, Daniel-Bertrand M, Buisson D-A, Tricard S, Lesot P, Coppel Y, Chaudret B, Feuillastre S, Pieters G, (2020) Tuning the reactivity of a heterogeneous catalyst using N-Heterocyclic Carbene ligands for C-H activation reactions. Angew Chem Int Ed 59:20879–20884

162. García-Zaragoza A, Cerezo-Navarrete C, Mollar-Cuni A, Oña-Burgos P, Mata J A, Corma A, Martínez-Prieto L M, (2022) Tailoring graphene-supported Ru nanoparticles by functionalization with pyrene-tagged N-Heterocyclic Carbenes. Catal Sci Technol 12:1257–1270

163. Martínez-Prieto L M, Ferry A, Lara P, Richter C, Philippot K, Glorius F, Chaudret B, (2015) New route to stabilize ruthenium nanoparticles with non-isolable chiral N-Heterocyclic Carbenes. Chem Eur J 21:17495–17502

164. Ernst J B, Muratsugu S, Wang F, Tada M, Glorius F, (2016) Tunable heterogeneous catalysis: N-heterocyclic carbenes as ligands for supported heterogeneous Ru/K-Al$_2$O$_3$ catalysts to tune reactivity and selectivity. J Am Chem Soc 138:10718–10721

165. Muratsugu S, Kityakarn S, Wang F, Ishiguro N, Kamachi T, Yoshizawa K, Sekizawa O, Urugagh T, Tada M, (2015) Formation and nitrile hydrogenation performance of Ru nanoparticles on a K-doped Al$_2$O$_3$ surface. Phys Chem Chem Phys 17:24791–24802

166. Liu J, Peng X, Sun W, Zhao Y, Xia C, (2008) Magnetically separable Pd catalyst for carbonylative Sonogashira coupling reactions for the synthesis of α,β-alkynyl ketones. Org Lett 10:3933–3936

167. Ranganath K V S, Kloesges J, Schäfer A H, Glorius F, (2010) Asymmetric nanocatalysis: N-heterocyclic carbenes as chiral modifiers of Fe$_3$O$_4$/Pd nanoparticles. Angew Chem Int Ed 49:7786–7789

168. Ikemoto S, Muratsugu S, Koitaya T, Tsuji Y, Das M, Yoshizawa K, Glorius F, Tada M, (2023) Coordination-induced trigger for activity: N-Heterocyclic Carbene-decorated ceria catalysts incorporating Cr and Rh with activity induction by surface adsorption site control. J Am Chem Soc 145:1497–1504

169. (a) Ikemoto S, Huang X, Muratsugu S, Nagase S, Koitaya T, Matsui H, Yokota G, Sudoh T, Hashimoto A, Tan Y, Yamamoto S, Tang J, Matsuda I, Yoshinobu J, Yokoyama T, Kusaka S, Matsuda R, Tada M (2019) Reversible low-temperature redox activity and selective oxidation catalysis derived from the concerted activation of multiple metal species on Cr and Rh-incorporated ceria catalysts. Phys Chem Chem Phys 21:20868–20877; (b) (15) Ikemoto S, Muratsugu S, Koitaya T, Tada M, (2022) Chromium oxides as structural modulators of rhodium dispersion on ceria to generate active sites for NO reduction. ACS Catal 12:431–441

170. Ernst J B, Schwermann C, Yokota G-i, Tada M, Muratsugu S, Doltsinis N L, Glorius F, (2017) Molecular adsorbates switch on heterogeneous catalysis: induction of reactivity by N-heterocyclic carbenes. J Am Chem Soc 139:9144–9147

171. Lewis R J, Koy M, Macino M, Das M, Carter J H, Morgan D J, Davies T E, Ernst J B, Freakley S J, Glorius F, Hutchings G J, (2022) N-Heterocyclic Carbene modified palladium catalysts for the direct synthesis of hydrogen peroxide. J Am Chem Soc 144:15431–15436

172. Sankar M, He Q, Morad M, Pritchard J, Freakley S J, Edwards J K, Taylor S H, Morgan D J, Carley A F, Knight D W, Kiely C J, Hutchings G J, (2012) Synthesis of stable ligand-free gold-palladium nanoparticles using a simple excess anion method. ACS Nano 6:6600–6613

173. Levratovsky Y, Gross E, (2016) High spatial resolution mapping of chemically-active self-assembled N-heterocyclic carbenes on Pt nanoparticles. Faraday Discuss 188:345–353

174. Cao Z, Derrick J S, Xu J, Gao R, Gong M, Nichols E M, Smith P T, Liu X, Wen X, Copéret C, Chang C J, (2018) Chelating N-heterocyclic carbene ligands enable tuning of electrocatalytic CO_2 reduction to formate and carbon monoxide: surface organometallic chemistry. Angew Chem Int Ed 57:4981–4985

175. Hou Y, Ji X, Liu G, Tang J, Zheng J, Liu Y, Zhang W, Jia M, (2009) Immobilization of palladium in N-heterocyclic carbene functionalized SBA-15 for the catalytic application in aerobic oxidation of benzyl alcohol. Catal Commun 10:1459–1462

176. Ranganath K V S, Schäfer A H, Glorius F, (2011) Comparison of superparamagnetic Fe_3O_4-supported N-heterocyclic carbene-based catalysts for enantioselective allylation. ChemCatChem 3:1889–1891

177. Mohapatra S, Chaiprasert T, Sodkhomkhum R, Kunthom R, Hanprasit S, Sangtrirutnugul P, Ervithayasuporn V, (2016) Solid–state synthesis of polyhedral oligomeric silsesquioxane-supported N-heterocyclic carbenes/imidazolium salts on palladium nanoparticles: highly active and recyclable catalyst. ChemistrySelect 1:5353–5357

178. Soulé J-F, Miyamura H, Kobayashi S, (2013) Copolymer-incarcerated nickel nanoparticles with N-Heterocyclic Carbene precursors as active cross-linking agents for Corriu−Kumada−Tamao reaction. J Am Chem Soc 135:10602–10605

179. Ganesan M, Freemantle R G, Obare S O, (2007) Monodisperse thioether-stabilized palladium nanoparticles: synthesis, characterization, and reactivity. Chem Mater 19:3464–3471

180. Solomonsz W A, Rance G A, Suyetin M, La Torre A, Bichoutskaia E, Khlobystov A N, (2012) Controlling the regioselectivity of the hydrosilylation reaction in carbon nanoreactors. Chem Eur J 18:13180–13187

181. Brust M, Walker M, Bethell D, Schiffrin D, Whyman R, (1994) Synthesis of thiol-derivatised gold nanoparticles in a two-phase liquid–liquid system. J Chem Soc Chem Commun 801–802

182. Rossi L M, Vono L L R, Garcia M A S, Faria T L T, Lopez-Sanchez J A, (2013) Screening of soluble rhodium nanoparticles as precursor for highly active hydrogenation catalysts: the effect of the stabilizing agents. Top Catal 56:1228–1238

183. Jacinto M J, Kiyohara P K, Masunaga S H, Jardim R F, Rossi L M, (2008) Recoverable rhodium nanoparticles: synthesis, characterization and catalytic performance in hydrogenation reactions. Appl Catal A 338:52–57

184. Altmann L, Kunz S, Bäumer M, (2014) Influence of organic amino and thiol ligands on the geometric and electronic surface properties of colloidally prepared platinum nanoparticles. J Phys Chem C 118:8925–8932

185. Yan M, Wu T, Chen L, Yu Y, Liu B, Wang Y, Chen W, Liu Y, Lian C, Li Y, (2018) Effect of protective agents upon the catalytic property of platinum nanocrystals. ChemCatChem 10:2433–2441

186. Liu B, Yao H, Song W, Jin, Mosa I M, Rusling J F, Suib S L, He J, (2016) Ligand-free noble metal nanocluster catalysts on carbon supports via "soft" nitriding. J Am Chem Soc 138:4718–4721

187. McKenna F-M, Anderson J A, (2011) Selectivity enhancement in acetylene hydrogenation over diphenyl sulphide-modified Pd/TiO_2 catalysts. J Catal 281:231–240

188. McKenna F M, Mantarosie L, Wells R P K, Hardacre C, Anderson J A, (2012) Selective hydrogenation of acetylene in ethylene rich feed streams at high pressure over ligand modified Pd/TiO_2. Catal Sci Technol 2:632–638

189. Mori A, Mizusaki T, Kawase M, Maegawa T, Monguchi Y, Takao S, Takagi Y, Sajiki H, (2008) Novel palladium-on-carbon/diphenyl sulfide complex for chemoselective Hydrogenation: preparation, characterization, and application. Adv Synth Catal 350:406–410

190. Makosch M, Lin W-I, Bumbálek V, Sá J, Medlin J W, Hungerbühler K, van Bokhoven J A, (2012) Organic thiol modified Pt/TiO_2 catalysts to control chemoselective hydrogenation of substituted nitroarenes. ACS Catal 2:2079−2081

191. Kahsar K R, Schwartz D K, Medlin J W, (2012) Liquid- and vapor-phase hydrogenation of 1-epoxy-3-butene using self-assembled monolayer coated palladium and platinum catalysts. Appl Catal A: Gen 445–446:102–106

192. Schoenbaum C A, Schwartz D K, Medlin J K, (2013) Controlling surface crowding on a Pd catalyst with thiolate self-assembled monolayers. J Catal 303:92–99

193. Kahsar K R, Schwartz D K, Medlin J W, (2013) Selective hydrogenation of polyunsaturated fatty acids using alkanethiol self-assembled monolayer-cated Pd/Al_2O_3 catalysts. ACS Catal 3:2041−2044

194. Pang S H, Schoenbaum C A, Schwartz D K, Medlin J W, (2014) Effects of thiol modifiers on the kinetics of furfural hydrogenation over Pd catalysts. ACS Catal 4:3123−3131

195. Kahsar K R, Schwartz D K, Medlin J W, (2013) Control of metal catalyst selectivity through specific noncovalent molecular interactions. J Am Chem Soc 136:520–526

196. Kahsar K R, Schwartz D K, Medlin J W, (2015) Stability of self-assembled monolayer coated Pt/Al_2O_3 catalysts for liquid phase hydrogenation. J Mol Catal A: Chem 396:188–195

197. Lien C-H, Medlin J W, (2016) Control of Pd catalyst selectivity with mixed thiolate monolayers. J Catal 339:38–46

198. Blanchette Z, Schwartz D K, Medlin J W, (2023) Directing reaction pathways on supported metal catalysts with low-density self-assembled monolayers. ACS Appl Nano Mater 6:9059−9069

199. Al Khulaifi F M, Alsunni Y A, Musgrave C B, Holewinski A, Medlin J W, (2023) Impact of pretreatment and thiol modifiers on the partial oxidation of glutaraldehyde using Pd/Al_2O_3. App Catal A: Gen 661:119229

200. Watson D J, Jesudason R J B J, Beaumont S K, Kyriakou G, Burton J W, Lambert R M, (2009) Heterogeneously catalyzed asymmetric hydrogenation of C=C bonds directed by surface-tethered chiral modifiers. J Am Chem Soc 131:14584–14589

201. Weng Z, Zaera F, (2014) Increase in activity and selectivity in catalysis via surface modification with self-assembled monolayers. J Phys Chem C 118:3672−3679

202. Wang Y, Ren J, Deng K, Gui L, Tang Y, (2000) Preparation of tractable platinum, rhodium, and ruthenium nanoclusters with small particle size in organic media. Chem Mater 12:1622–1627

203. (a) Azmat M U, Guo Y, Guo Y, Wang Y, Lu G, (2011) An easy and effective approach towards heterogeneous Pt/SiO2-cinchonidine catalyst system for enantioselective hydrogenation of ethyl pyruvate. J Mol Catal A: Chem 336:42−50; (b) Huang Y, Xu S, Lin V S Y, (2011) New strategy for enantioselective heterogeneous catalysis: immobilization of both metal nanoparticles and chiral modifiers on mesoporous silica nanoparticles. ChemCatChem 3:690−694